Universidad de Concepción
Dirección de Postgrado
Facultad de Ciencias Físicas y Matemáticas - Programa de Magíster en Ciencias con mención en
Física

When groups enter clusters: Insights from cosmological simulations
(Cuando grupos entran en cúmulos: Perspectivas desde simulaciones cosmológicas)

Tesis para optar al grado de Magíster en Ciencias con mención en Física

NELVY CRISTINA CHOQUE CHALLAPA
CONCEPCIÓN-CHILE
2016

Profesor Guía: Dr. Michael Fellhauer
Departamento de Física
Facultad de Ciencias Físicas y Matemáticas
Universidad de Concepción

Resumen

En el paradigma actual de formación de estructura, la materia oscura colapsa en halos en una manera ascendente. Pequeños objetos se forman primero y con el tiempo ellos se fusionan en sistemas cada vez más grandes. De este modo, los grupos y cúmulos se convierten en lugares importantes donde las galaxias están evolucionando. Más aún, de varios estudios se sabe que una fracción significante de galaxias están siendo acretados en cúmulos dentro de sistemas más pequeños como grupos, señalando la importancia no sólo del entorno del cúmulo en la evolución de una galaxia, sino también del grupo. Adicionalmente, observaciones indican que algunas galaxias de cúmulos han estado sujetas a transformaciones previas dentro del entorno de un grupo, apoyando la idea de una influencia continua del entorno en las galaxias. En esta tesis, se estudian las consecuencias del entorno del cúmulo y grupo en la evolución de halos galácticos de materia oscura analizando un set de simulaciones cosmológicas de N-cuerpos de alta resolución.

El foco de esta tesis es la pérdida de masa de marea de las galaxias en grupos, y en las consecuencias de éste mientras está cayendo al entorno de un cúmulo. Los resultados muestran que el grupo es capaz de causar pérdida de masa severa en algunos de sus halos miembros. Más aún, cuando los grupos llegan a ser parte del cúmulo se produce un incremento en la pérdida de masa causado por las fuertes fuerzas de marea que los grupos y sus miembros pueden experimentar dentro de este entorno. Por otra parte, la pérdida de masa de los halos miembros de grupos depende del tipo de órbita que tienen en su grupo. Aquellos hundiendose muy cerca del centro de su halo anfitrión vienen ligados al destino de su grupo, mientras que aquellos que miembros de grupos no teniendo este comportamiento en su órbita tienden a perder más masa, ya que ellos están más susceptibles a las mareas del grupo mientras orbitan.

La evolución temporal de los halos dentro de su halo anfitrión también es analizada, poniendo una atención específica a a la evolución de halos miembros de grupos que escapan de su grupo. Por consiguiente, se analiza cuando y porqué estos halos son liberados, mientras que otros permanencen como miembros de un grupo. Se encuentra que la distancia que tienen los halos miembros respecto de su grupo, cuando éste pasa por el pericentro en el cúmulo es un parámetro crucial determinando la probabilidad de escape. Por lo tanto, estos resultados apoyan la noción de grupos poblando un cúmulo con galaxias previamente afectadas o "pre-procesadas".

Abstract

In the current standard paradigm for structure formation, dark matter collapses into halos in a bottom-up fashion. Small objects form first and over time they merge into larger systems. Thus, groups and clusters become important places where galaxies evolve. Moreover, from several studies we know that a significant fraction of galaxies is being accreted into the cluster within smaller systems, suggesting that cluster galaxies may be pre-processed by these systems. In addition, observations indicate that cluster galaxies have been subject to transformation processes in group environments, supporting the notion of continuous environmental influence on galaxies. In this thesis, the effect of the cluster and group environments on the evolution of galactic dark matter halos was studied using a set of high-resolution, N-body cosmological simulations.

The focus on this thesis is on the tidal mass loss of group galaxies, and the consequences of their group infalling into the cluster environment. The result shows that the group is able to cause severe mass loss in some of their members, which highlights that the tidal field within groups can be very important for the mass loss of some cluster galaxies. Moreover, when they become part of the cluster there is an enhancement on the mass loss caused by the strong tides that the group and their member halos can experience inside this environment, supporting the notion of continuous environmental influence. However, the mass loss of group-member halos is depending on the orbital behaviour that they have within their host group. Those ones sinking close to the host centre become tied to the fate of their host group, meanwhile those group-member halos do not having this behaviour typically tend to lose more mass, as they are more susceptible to the group tides while orbiting.

The temporal evolution of halos within their host group was also analysed, paying specific attention to the evolution of group-member halos that escape from their host. This was extended to study when and why the escaping halos are being released, while other remain as group-members. It was found that the group-centric distance of the halo at pericentric passage of the group in the cluster is a crucial parameter for determining the escape probability. Moreover, this seems that tidally damaged halos are being released, and thus lending support to the notion of groups populating a cluster with pre-processed galaxies.

Acknowledgements

My thanks and appreciation goes out to all of these people;

Contents

List of Tables

List of Figures

Chapter 1

Introduction

1.1 Structure formation

For many decades, trying to understand the formation and evolution of structure on the largest observable scales of the Universe has been a challenge for astrophysicists. But since the detection of the CMB (Cosmic Microwave Background) radiation we have learned a great deal more about this. Tiny fluctuations in temperature have been discovered that are measures of the primordial density fluctuations of matter in the early Universe. The CMB is the leftover radiation from an early stage in the development of the Universe, and its discovery is considered a landmark test of the Big Bang model. In this accepted theory, the evolution of the Universe began ~ 13.7 billion years ago with an initial moment known as the Big Bang. Then, shortly after this event, an expansion epoch starts, known as inflation and the size of the universe started expanding exponentially. The primordial density fluctuations were then amplified to a macroscopic scale. As the Universe was dominated by photons and neutrinos (i.e. radiation), the growth of the density perturbations was retarded, but after that the energy density of the Universe transitioned to being dominated by matter. In this epoch structure formation began through gravitational collapse of cold dark matter. However, the hot, ionized baryons remained tightly coupled to the radiation field and were unable to further collapse until the Universe cooled sufficiently, at which point the baryons were able to collapse into the early
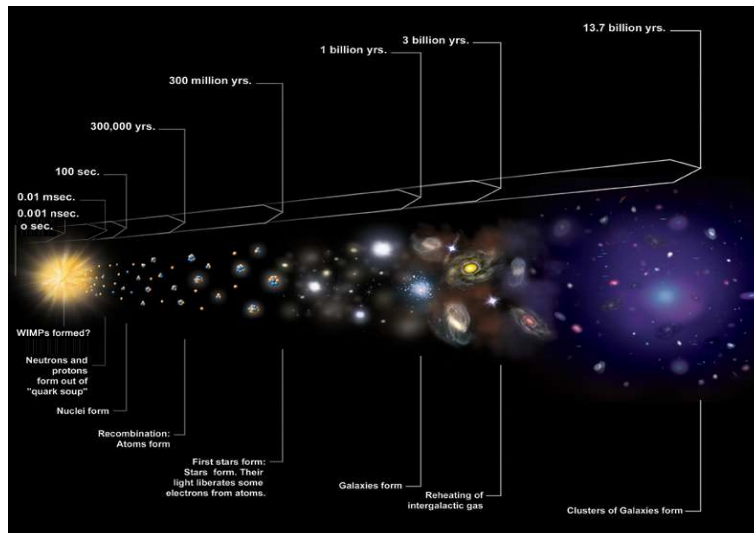
Figure 1.1: Illustration of the Universe's evolution in different epochs (image taken from NASA/CXC/M.Weiss).

structures formed by cold dark matter, around 300,000 years after the Big Bang. This process continues until today, with both dark matter and baryons undergoing gravitational collapse. Fig. 1.1 illustrates the cosmic evolution of the Universe through the different epochs.

1.1.1 ΛCDM cosmology

The most widely accepted model to describe the Universe is the ΛCDM model[1], also called the standard model of cosmology. In this model the Universe is described by a spatially flat space-time with a matter/energy content comprised of cold dark matter (CDM), baryonic matter, radiation and a cosmological constant (Λ), which is causing the expansion of the Universe to accelerate at the present epoch. This model also postulates the hierarchical formation of structures. One of the tests of this cosmological model is the CMB radiation, supporting the idea that the Universe in its early stage was homogeneous, with small quantum fluctuations that are the origin of the primordial density fluctuations of matter. Particularly from the measurement of the fluctuations in the temperature of the CMB, it has been possible to measure several cosmological parameters, such as the density of matter and energy, the Hubble constant, the slope of the primordial power spectrum, and others. In this context the universe is composed

---

[1]Other alternative models have been proposed challenging the assumptions of ΛCDM, such as modified gravity theories like MOND (MOdified Newtonian Dynamics), for example.

by a small fraction of baryonic matter $\Omega_b \sim 0.04$ (at the present time), which is the visible
Universe that we know. But the rest of the matter content is an "invisible" component called
cold dark matter, containing a present-day fraction of $\Omega_{dm} \sim 0.2$ of the total matter, whose
existence is inferred from its gravitational effect. In this ΛCDM model the largest constituent
is dark energy $\Omega_\Lambda \sim 0.76$ (at the present time), a mysterious energy present throughout space,
producing a negative pressure, causing an accelerated expansion of the Universe. Some of the
current measurements of the cosmological parameters and their contribution are listed in the
table 1.1 (taken from "Plank 2015 results. XIII Collaboration Cosmological parameters" Planck
Collaboration et al. (2015)).

Component	Parameter	Value	Error
Baryon matter density	$\Omega_b h^2$	0.02230	0.00014
Dark matter density	$\Omega_{dm} h^2$	0.1188	0.0010
Dark energy density	Ω_Λ	0.6911	0.0062
Hubble constant	H_0	67.74 $Kms^{-1}\ Mpc^{-1}$	0.46
Scalar spectral index	n_s	0.9667	0.0040
Fluctuation amplitude at $8h^{-1}Mpc$	σ_8	0.8159	0.0086

Table 1.1: Parameters listed from the Planck Collaboration. Cosmological parameters 68% confidence
limits for the base ΛCDM model from Planck CMB power spectra, in combination with lensing
reconstruction and external data. Here h is related to the Hubble constant by the equation $H_0 = 100h$
$(Km/s)/Mpc$.

1.1.2   DM halo formation

The hierarchical theory of structure formation aims to address how DM halos form. In a
general description this process is explained by taking into account that in the early stages
of the Universe, as incorporated into the ΛCDM model, there were tiny density fluctuations,
and so there were overdense regions and underdense regions (as we see in the CMB). The
overdensities then collapsed under their own gravity. During this accretion process, however,
the Universe was expanding, so an effective "repulsive force" was acting in these overdense
regions. At some point the self-gravity of the overdensity becomes sufficiently large that the
structure starts collapsing and bound objects are formed. The radius at which the overdense
region starts to collapse is called the *turnaround radius* (r_m).

During the process of gravitational collapse, the potential through which the collisionless dark matter particles move will undergo both phase mixing and violent relaxation (Lynden-Bell, 1967) to reach a final configuration with a specific virial radius $r_{vir} = r_m/2$. This virialization process, as it is called, gives rise to an approximately stable, near-equilibrium dark matter halo, where this halo is supported against its own self-gravity by the random motions of its particles (for more detail see Padmanabhan 1993). A full description of the formation of halos through non-linear gravitational collapse of dark matter, both in individual halos and the subsequent fusion of multiple halos to give rise to more massive objects, is highly complex. Thus, it is necessary to use numerical N-body[2] simulations to get more insights into this process.

1.1.3 DM Halo properties

Some of the evidence proposed for the existence of dark matter halos are the rotation curves (measurement of the orbital velocities of stars and gas versus their radial distance from that galaxy's centre) of galaxies. Since the study of velocity curves of edge-on spiral galaxies done by Vera Rubin in the 1970s (results in Rubin, Ford & . Thonnard (1980)), there has been substantial effort to understand some discrepancies of the observations with theoretical predictions. This discrepancy or galaxy rotation problem is described by assuming that without large amounts of mass throughout the halo, the rotational velocity would decrease at large distances from the centre of the galaxy. From observations of the line emission of neutral atomic hydrogen in spiral galaxies, however, we see a different curve from that which we would expect, i.e., the rotation curve of most spiral galaxies flattens out (as we can see in the fig. 1.2) suggesting that the dominant matter component is an extended dark halo). As the rotational velocities do not decrease at larger distances, the absence of visible matter implies either that there is matter that we cannot observe (dark matter) or that the theory of motion under gravity is not correct.

The flattening of the rotation curve was first explained by assuming a spherical halo, as in this

---

[2]N-body simulation basically is a simulation of a dynamical system of particles, under the influence of the gravitational force. Usually in cosmology these simulations are used to study the processes of non-linear structure formation, leading to galaxy filaments and galaxy halos.
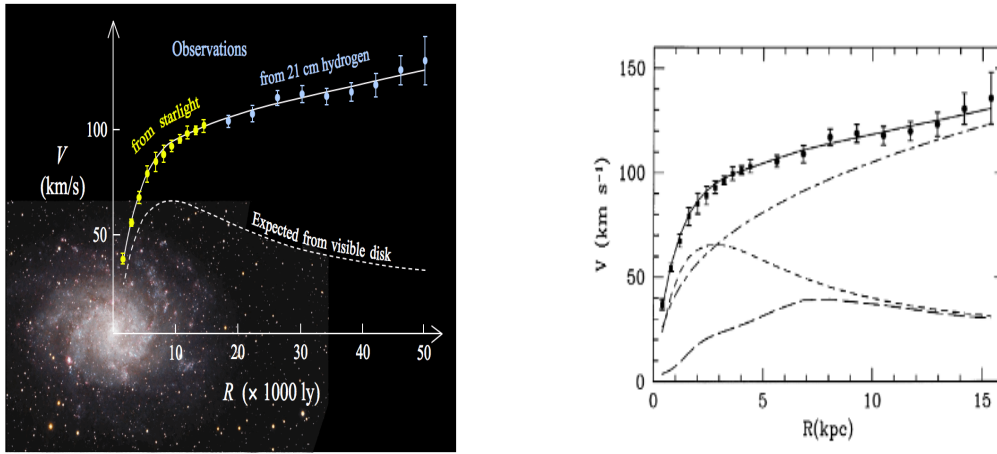
Figure 1.2: *Left:* Image showing an example of a typical rotation curve (blue and yellow points) for a spiral galaxy and the predicted curve (dashed white line) for the visible matter in the galaxy. The discrepancy implies the presence of a kind of "dark matter". *Right:* Rotation curve for M33 (points). Compared to the halo contribution (dot dashed line), the stellar disc (short-dashed line) and the gas contribution (long-dashed line), (Corbelli & Salucci, 2000).

case the internal mass distribution is fully described by a density profile $\rho(r)$. An isothermal profile was proposed as the halo model, i.e., assuming an isothermal sphere with a profile $\rho(r) \propto 1/r^2$. This profile was used to model a virialized dark matter halo and clearly implies a constant velocity dispersion, which further implies a constant temperature profile for the hot halo gas. However, in this isothermal model, many effects cause deviations from the isothermal profile predicted by the simple self-similarity model (Mo, van den Bosch & White (2010)), such as: (i) the collapse may never reach an equilibrium state in the outer reaches of the halo; (ii) non-radial motion may be important and (iii) mergers associated to hierarchical halo formation will disrupt the halo profile. The importance of such effects on the final density profile is difficult to model analytically. However given the progress of numerical simulations, particularly the use of high-resolution N-body simulations of the structure formation like those performed by Navarro, Frenk & White (1996, 1997), it appears that the density profile of halos are not well approximated by isothermal profiles but rather have gently changing logarithmic slopes, known as an NFW profile:

$$\rho(r) = \frac{\rho_s}{(r/r_s)(1 + r/r_s)^2} \tag{1.1}$$

Here, r_s is the scale radius and ρ_s is the characteristic density. This profile shows that the density of the simulated DM halos are shallower than r^{-2} at small radii and steeper at large radii. Also from this profile we can get the enclosed mass in a radius r, given by:

$$M(r) = 4\pi\rho_s r_s^3 \left[ln\left(\frac{r_s + r}{r_s}\right) - \frac{r}{r_s + r} \right] \qquad (1.2)$$

From this mass profile it is possible to obtain the circular velocity curve for the halo,

$$V^2(r) = 4\pi\rho_s G r_s^3 \frac{1}{r} \left[ln\left(1 + \frac{r}{r_s}\right) - \frac{r/r_s}{1 + r/r_s} \right] \qquad (1.3)$$

Then using the fact that the virial mass (M_{vir}) of the halo is related with its virial radius (r_{vir})

$$M(r = r_{vir}) = \frac{4}{3}\pi\Delta\rho_{crit}r_{vir}^3 \qquad (1.4)$$

Here the Δ parameter is the density contrast. Then the density profile can be written as

$$\frac{\rho(r)}{\rho_{crit}} = \frac{\delta_c}{(cr/r_{vir})(1 + cr/r_{vir})^2} \qquad (1.5)$$

This equation defines the concentration parameter $c = r_{vir}/r_s$. The virial radius r_{vir} is usually approximated by R_{200} which is defined as the radius within which the average density is 200 times the critical density of the Universe. Through the parameter δ_c, the characteristic density is related to the concentration parameter as:

$$\delta_c = \frac{\Delta}{3} \frac{c^3}{ln(1+c) - c/(1+c)} \tag{1.6}$$

Thus for a given cosmology, the NFW profile is completely characterized by its mass and the concentration parameter. The NFW profile is widely used, but other high resolution numerical simulations report deviations from this profile (e.g. Navarro et al., 2004; Merritt et al., 2005). DM halos seem to be slightly better described by an Einasto density profile with a form:

$$\rho(r) = exp(-Ar^\alpha) \tag{1.7}$$

In this profile α denotes the curvature of the profile. However the simple form of the NFW profile is accurate to within 10%-20% (Benson (2010) review) making it still useful.

1.1.4   Galaxy formation

In the current model of galaxy formation, galaxies are formed and reside inside of DM halos. White & Rees (1978) proposed a two-stage theory for galaxy formation, where dark halos form first through hierarchical clustering and then the luminous content of galaxies results from cooling and condensation of gas within the potential wells provided by these dark halos (the main ideas of this model are in the modern theory of galaxy formation). In a general description, this process is explained by assuming that in the early stages of the Universe, the baryonic matter was in a gaseous form, and that this baryonic material was then dragged along by the gravitationally dominant dark matter such that dark matter halos accreted baryonic material. The joint accretion[3] of dark matter and baryonic matter into the potential well of

---

[3]This matter accretion process and the subsequent evolution to form a galaxy, through star formation and the formation of its central black hole, is a complex process that is not well understood (more detail in Benson (2010); Somerville & Davé (2015).

the halo produces an increase in the temperature of the baryons, and the temperature increases until an equilibrium stage is reached. Subsequently the evolution of these two components is very different, with the baryonic matter losing thermal energy due to the cooling by radiation processes, while the dark matter, being collisionless, does not experience this kind of process. As the gas loses energy, it collapses in a dissipative way to the center of the halo until it is supported by its angular momentum. Once gas has collapsed into the inner region of the halo, it may become self-gravitating, i.e. dominated by its own gravity rather than that of the DM. In this collapsed structure molecular clouds (MC) are formed and subsequently give rise to star formation and thereby the formation of a galaxy. However, many details of these processes are not well understood yet and, moreover, most cosmological simulations are not able to resolve even the scales on which MCs form, much less individual stellar cores.

1.1.5 Hierarchical scenario

In the current hierarchical scenario of structure formation, halos first form as small objects and grow more massive over time. The formation history of a dark matter halo can then be described by a "merger tree" as illustrated in Figure 1.3 (Jiang & van den Bosch, 2014). This scenario plays an important role in the current theory of galaxy formation and evolution. In CDM models the growth of a massive halo is due to merging of a large number of small halos and, to a good approximation, such mergers can be thought of as a smooth accretion. When two similar mass halos merge, violent relaxation transforms the orbital energy of the progenitors into the internal binding energy of the quasi-equilibrium remnant (Mo, van den Bosch & White, 2010). Furthermore, during the merger the associated gas is shock-heated and settles back into hydrostatic equilibrium in the new halo. If the halos contain central galaxies, they will merge in a "violent process", allowing a new galaxy to form. In the case that two halos of very different mass are merging, the dynamical process is less violent. The smaller system or subhalo orbits within the main halo for a time, during which processes such as dynamical friction and tidal effects determine their eventual fate. This will be explained in more detail later. In this process of build-up, groups and clusters of galaxies are formed.

As the resolution of numerical simulations improves, the ability to determine substructures has also improved, with more subhaloes or substructures being identified (e.g. Springel et al., 2008). One of the classic problems with the standard cosmological model using cold dark matter (CDM), however, is the large quantity of subhalos that are shown in simulations in comparison to the relatively low quantity of satellite galaxies that have been observed (Moore et al., 1999a; Klypin et al., 1999; Bullock, 2010) in the Local Group. This is known as the "missing satellites" problem. To address this question many solutions have been proposed, including the possibility that the smallest DM halos in the Universe are extremely inefficient at forming stars, but this problem is still not well understood.
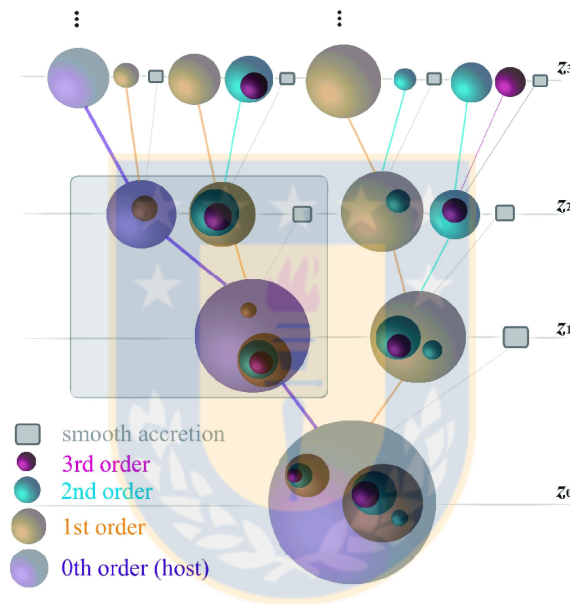
Figure 1.3: "Merger tree" schema, illustrating the merger history of a dark matter halo. It shows four different epochs, starting from the early progenitor halos to their merger by redshift $z = 0$. Merger histories of DM halos play an important role in the hierarchical theory of galaxy formation and evolution. Image taken from Jiang & van den Bosch (2014).

1.2   Galaxies

It was not until the 1920s that we became convinced that the *nebulaes* are indeed galaxies, and with the progress of observational techniques and the theories of structure formation it is now possible to have a wide perspective on galaxy structure and morphology and how these are formed (as was pointed out in the previous sections).

1.2.1 Classification

With the large variety in morphologies, sizes, mass and content of galaxies, it would seem to be increasingly difficult to fit them into the standard classification scheme developed originally by Hubble (1936). Basically this sequence distinguishes galaxy types[4] based on their morphology, consisting of two main types of galaxies: ellipticals and spirals (with a further division of spirals into those with bars and those without bars). In addition there are lenticulars and a fourth class containing galaxies with an irregular appearance. The figure 1.4 shows the different types. This classification often refers to ellipticals and lenticulars as "early-type", whereas spirals and irregulars make up the class of "late-type" galaxies. These references to "early" and "late" should not be interpreted as reflecting a property of the galaxy's evolutionary state. Also there are galaxies which do not readily fit into the scheme, as it is based on bright nearby galaxies. Additional types, such as low surface brightness galaxies, dwarf galaxies, ultrafaint galaxies, spheroids and galaxies altered by the environment need to be also taken into account in this galaxy-zoo. Thus, it is not only important to explain the large categories of galaxies, but also the complex transitions between types and their dependencies on each other.

1.2.2 Environmental dependency

At the largest scales, galaxies are distributed in a complex web of filaments and sheets surrounding large empty voids, called the cosmic web. They can reside in different environments, which can be correlated with the properties of the galaxy, such as their star formation (SF) histories, masses and morphologies. Massive, passively evolving spheroids dominate the cluster cores, while in field regions, galaxies are typically low-mass, star-forming, and disk-dominated. These relations of the local environment with the properties of galaxies have been quantified through the classic morphology-density relation (e.g. Dressler, 1980; Bouchard, Da Costa & Jerjen, 2009) and SF-density relations (e.g. Poggianti et al., 2008; Ziparo et al., 2014). It is still unclear if these trends with the environment are a direct result of the initial conditions

---

[4]Elliptical galaxies are composed by a spheroidal-like bulge and have no disk. Lenticulars are essentially elliptical galaxies with a very thin disk which gives them the shape of a lentil. Spiral galaxies have a central bulge surrounded by an extended disk with a pattern of spiral arms.
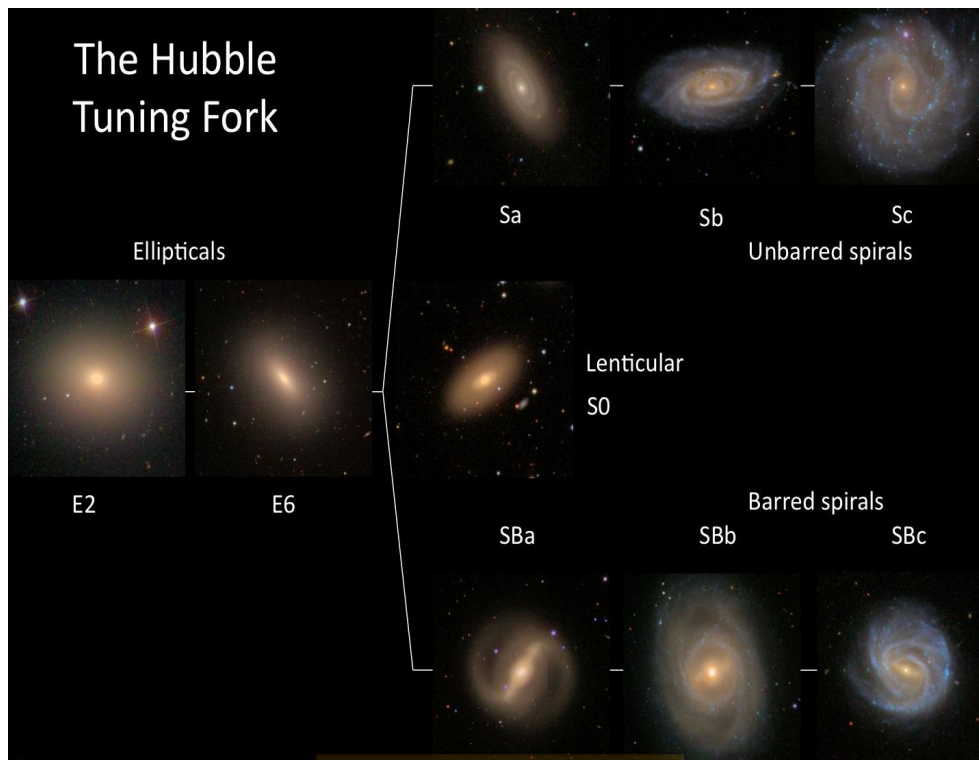
Figure 1.4: Examples of different types of galaxies in the Hubble sequence.

in which galaxies are formed or if they are produced by later interactions of galaxies with the environment. Thus, several mechanisms have been proposed to explain their internal and morphological transformations, such as ram-pressure stripping (Gunn & Gott, 1972), mergers (Toomre & Toomre, 1972), harassment (Moore et al., 1999b) and other mechanisms. The importance of these processes have been taken into account to explain for example the quenching of star formation.

As galaxies are believed to form and reside in dark matter halos, several parameters are used to characterize the environment of a galaxy and to relate galaxy properties to the properties of the host halo (such as halo mass, spin, shape), and those related to the superhalo scales (such as mass of the filament or sheet in which the halo is embedded, or the mass overdensity on scales significantly larger than an individual halo). Furthermore, in the context of galaxy populations within DM halos (ignoring the effect on superhalo scales), the influence of the environment is usually analysed by considering central[5] and satellites galaxies separately (more detail in Mo,

---

[5]The definition of a central galaxy used in most studies, is the brightest or the most massive galaxy within a dark matter halo. However, both semi-analytic simulations and analysis of observations at low redshift indicate that a non-negligible fraction of galaxies that lie at the deepest point within the potential well are not in fact

van den Bosch & White 2010).

- **Centrals**. More massive central galaxies are expected to reside in more massive halos, and the redder and more centrally concentrated they are, the more likely they are to be ellipticals. The spins and the shapes of dark matter halos (Bett et al., 2007) are expected to have some impact on the properties of central galaxies. For example the distribution of halo spin is a basic input to model galaxy formation, (e.g. Cole et al., 2000) but these parameters are not easily accessible to observations. It is important to keep in mind that the central regions of DM halos are special environments in themselves. They are the repositories of low angular momentum material and of massive objects brought to the center of the potential well by dynamical friction. Consequently central galaxies are exposed to a number of processes that satellites are not.

- **Satellites**. Such galaxies are expected to be more susceptible to environmental effects such as harassment, tidal stripping, ram-pressure stripping, and dynamical friction. All these processes are not only expected to affect the star formation, but also transform the morphology, e.g. transforming disk components into a more spheroidal morphology. This change in the properties has been deduced by studying for example the properties of galaxies located in halos at different distances from its center. To further test if the properties of satellite galaxies are influenced differently by the environment (van den Bosch et al., 2008) compared the colours and concentrations of satellite galaxies to central galaxies of the same stellar mass, adopting the hypothesis that the latter are the progenitors of the former. What they found is that, on average, satellite galaxies are redder and more concentrated than central galaxies (for the same stellar mass) indicating that satellite-specific transformation properties do indeed operate. These differences between satellite and central galaxies may be explained by a fading model in which the star formation decreases after a galaxy becomes a satellite, causing a reddening of the galaxy (Weinmann et al., 2009).

---

the most luminous or most massive galaxies in their halos (as is pointed out in Knobel et al. (2013), more detail of this definition is discussed in Carollo et al. (2013)).

Whether or not galaxy properties depend on the environment at superhalo scales is less clear, as on these scales the dynamical times are longer than or comparable to the Hubble time, so there has not been enough time to induce an environmental dependence on these scales by gravitational processes. Furthermore, the processes affecting the evolution of galaxies is principally in galaxy groups and clusters.

1.3   Galaxy groups

Galaxy groups are one of the larger systems of gravitationally bound objects to have arisen thus far in the process of cosmic structure formation. These systems are a concentration of galaxies, embedded in an extended dark matter halo, where the galaxies are bound due to their mutual gravitational attraction. A group contains typically fewer bound galaxies, but its definition is still debated (as is also true for galaxy clusters). For example, is there a limit in the minimum number of galaxy members? Therefore, though clusters are larger than groups, there is no explicit sharp dividing line between them. But the importance of groups lie in that most of the galaxies reside in these gravitationally bound structures (e.g. Merchán & Zandivarez, 2005; Yang et al., 2005), so part of their evolution takes place in these environments, and since groups are regions of intermediate density, the effect of this environment can be compared with galaxies evolving in cluster and field regions.

Typically groups are selected having a typical size of a few megaparsecs with total masses covering the range $10^{12.5} - 10^{14} h^{-1} M\odot$ (but again this ranges depends on the classification). They can also be classified depending on their configuration as for example in compact groups (e.g. Hickson 1982) and fossil groups. Since these systems have sufficiently high density, yet rather low velocity dispersions, some of the processes affecting the evolution of galaxies occur more frequently in groups, such as mergers or morphology transformations, in comparison with cluster regions. Thus, one expects galaxy-galaxy interactions to be more dominant in groups. Furthermore, from current studies we know that most galaxies have been affected by these dense local environments prior to their accretion into clusters (Cortese et al., 2006).

1.4 Galaxy cluster

Clusters of galaxies are the most massive bound objects in the Universe. These systems, like groups, are an aggregation of galaxies, but they are more populous and denser systems containing a large number of galaxies in the range of a few galaxies up to thousands of them. In general, clusters have a mass in the range of $10^{14} - 10^{15} M_\odot$, and with a rich population of early-type galaxies in comparison to low density regions (similarly for groups). In addition, galaxies in the inner regions of these dense environments, are on average redder, less gas-rich, and have lower specific star formation rates both at $z \sim 0$ and at higher redshift (e.g. Lewis et al., 2002; Balogh et al., 2002). This suggests that the cluster environment is capable of perturbing the morphology and star-formation (Gunn & Gott, 1972; Poggianti et al., 2001). Particularly these effects are more severe in the core of the cluster. Interactions of galaxies, however, tend to take place while they are being accreted into the cluster, most of the times being part of groups (as was pointed out in the previous section). In this context, galaxy groups represent natural sites for a *pre-processing* stage in the evolution of a cluster.

1.5 Pre-processing and Post-processing

Galaxies reside in different environments, as the hierarchical structure formation paradigm makes clear. They and their DM halos tend to form early, then merge to form large groups and clusters. Before they become members of clusters, many galaxies experience high-density environments, as members of groups or by forming within large-scale filaments. In this context, the mechanisms affecting the evolution of galaxies, before infall into the cluster is referred to as a *pre-processing* stage (e.g. Fujita, 2004; Vijayaraghavan & Ricker, 2013). Cosmological simulations can provide the fraction of subhalos that previously were in groups, for example from the analysis of the Millennium II simulations (Springel et al., 2005). With semi-analytical models it has been found that large fractions of group and cluster galaxies (in particular those of low stellar mass) have therefore been pre-processed as satellites of groups with mass $\sim 10^{13} M_\odot$ (De Lucia et al., 2012). Some studies suggest that the percentage of galaxies that were accreted

through groups is in the range of $25-45\%$ (McGee et al., 2009). An interesting piece of evidence is the case of the star-bursting group falling into Abell 1367 (Cortese et al., 2006), where they found peculiar morphologies and unusually high $H\alpha$ emission, making this group the region with the highest density of star formation activity. $H\alpha$ imaging observations reveal extraordinary complex trails of ionized gas behind the galaxies (as shown in fig. 1.5). The properties found in this group suggest that environmental effects within infalling groups may represent a pre-processing step of galaxy evolution during the high redshift cluster assembly phase. This is one aspect of the study described in this thesis.

When galaxies, being part of groups, fall into clusters, they are not dissociated immediately. The gas and dark matter in these galaxies interacts with the intracluster medium, affecting the local environment experienced by group member galaxies. This step is referred to as the *post-processing* stage. Studies from simulations show for example that a groupcluster merger can affect cluster galaxies themselves: galaxies in clusters that undergo one or more major mergers in their evolutionary history can be subject to more transformation processes than those in clusters that evolve quiescently (more detail Vijayaraghavan et al. 2013).

1.5.1   Physical processes in dense environments

Galaxies in groups and cluster environments can be affected in different ways, (i) due tidal interaction with other group/cluster members and with the (group/cluster) potential, (ii) dynamical friction, which causes galaxies to sink to the center of dark matter halos, and (iii) interactions with the intracluster/group medium. All these different effects influence the morphology of a galaxy and its internal processes (more detail see Benson (2010) and references therein).

Galaxy Mergers

The gravitationally bound interactions of dark matter halos (and their galaxies) typically result in a transformed galaxy. This interaction requires a dissipative process, in a way that close encounters between two systems can lead to a merger (e.g the Antennae galaxies). Mergers
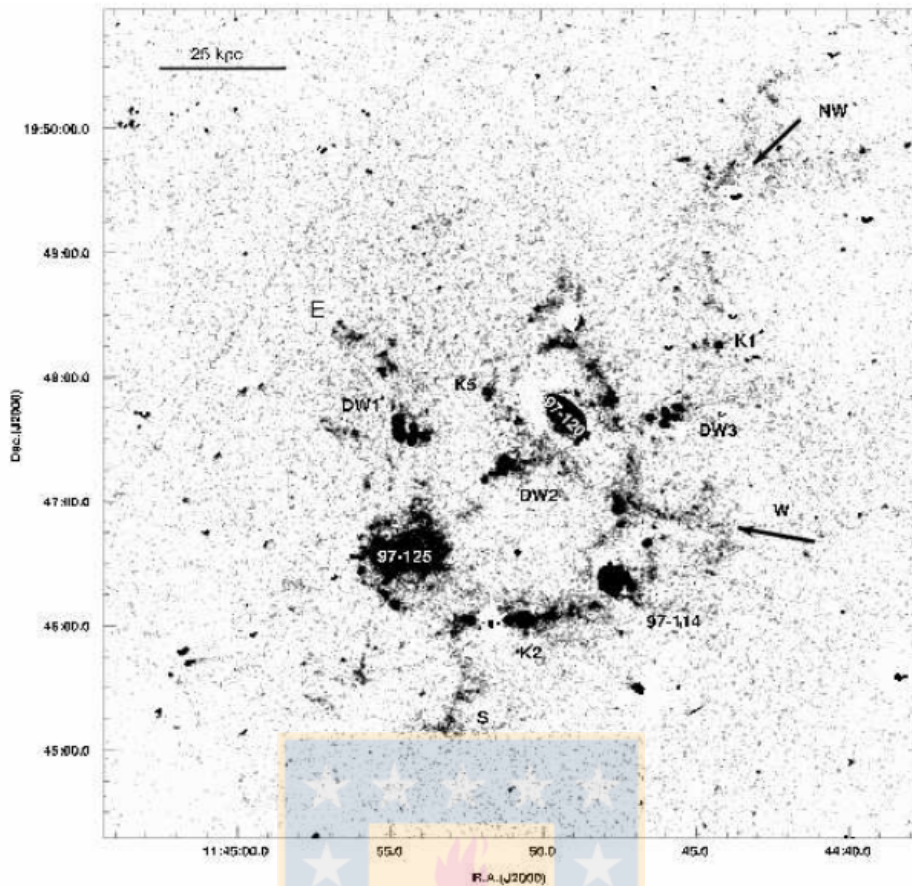
Figure 1.5: $H\alpha$ images of a blue infalling group (BIG) obtained with the TNG telescope. It reveals a spectacular $H\alpha$ filamentary structure on top of the star forming knots. Also multiple loops of ionized gas appear, making these among the most extended low-brightness $H\alpha$ emission. One stream (labeled NW) extends from the northern edge of the frame to the dwarf galaxy DW3, with an extension of $\sim$ 100kpc. The second and brightest one(W) apparently traces a loop around the galaxy CGCG97-120 and seems connected to the bridge (labeled K2) between CGCG97-114 and CGCG97-125. Image and description of it was taken from Cortese et al. (2006).

are effective in systems with an orbital velocity smaller than or comparable to the internal velocities of the galaxies. Thus, it galaxy mergers more commonly occur in galaxy groups. During the encounter, the extended halos may merge into a common halo, and eventually the galaxies may merge also (however not necessarily at same time). They orbit in the common halo until dynamical friction and tidal interactions remove sufficient orbital energy, causing the merger (Mo, van den Bosch & White, 2010). During a merger the gas is driven towards the galaxy center, cools rapidly and undergoes a burst of star formation. In addition tidal tails are observed in a merger of disk galaxies, as is shown in Figure 1.6. The same is seen in numerical simulations.

In recent years the effects of galaxy mergers have been widely studied, primarily trying to explain galaxy morphology: whether elliptical galaxies have formed from mergers, as proposed by Toomre & Toomre (1972), and widely tested with simulations (e.g. Di Matteo, Springel & Hernquist, 2005).

Ram pressure stripping

When galaxies move through the intracluster medium (ICM), they experience a significant drag force from the ICM. If the drag force is great enough, it may remove/strip the hot and cold gas from the infalling galaxy (Gunn & Gott, 1972). This consequently leads to quenched star formation. Hence ram-pressure stripping could explain why dense environments, such as galaxy clusters, have a deficit in gas-rich star-forming galaxies, suggesting their importance for transforming spirals into SO galaxies (van der Bergh 1976). However, other studies are questioning whether ram-pressure stripping can ultimately transform spirals into lenticular galaxies (Boselli & Gavazzi, 2006). From observations (an interesting observed example is in Ebeling et al. 2014) and simulations it is possible to see evidence of stripped gas and consequently a quenching of the star formation.

Tidal disruption

Subhalos (and their galaxies) orbiting in a larger host halo experience tidal forces, which may strip away the outer regions, or in extreme cases, entirely disrupt the galaxy resulting in a stellar stream, such as the recent example of a tidally disrupted dwarf spheroidal galaxy around the nearby spiral galaxy NGC 253 (Toloba et al., 2016), and the case of a tidally disrupted dwarf galaxy by the Hydra I cluster (Koch et al., 2012). Some studies suggest that the formation of UCD galaxies could be the result of a tidal disruption process, indicating that these would be the remnant nuclei of dwarf galaxies whose extended stellar component and DM halo have been both entirely disrupted by gravitational interactions within the host cluster (Pfeffer & Baumgardt, 2013; Kazantzidis, Moore & Mayer, 2004).

Also some studies point out that particles in an orbiting satellite that are on prograde orbits are more easily stripped than those on radial orbits which are in turn more easily stripped than those on retrograde orbits (Read et al., 2006).
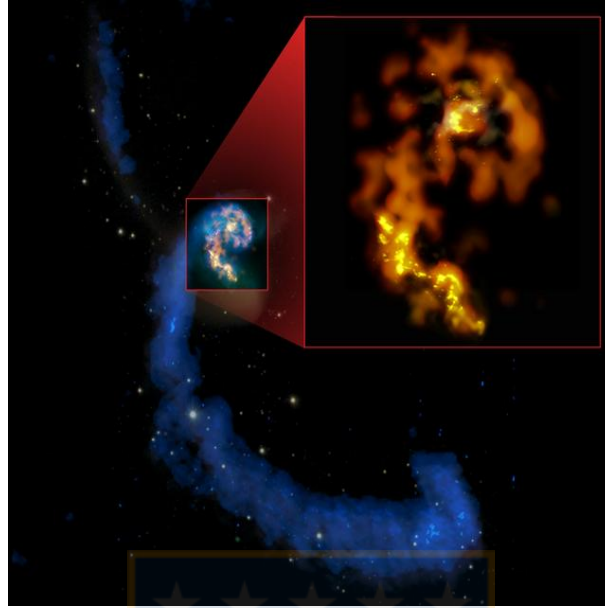
Figure 1.6: Famous example of two disk galaxies NGC 4038/4039 merging. Image composed by multiple wavelengths, showing their tidal tails in radio (blue), past and recent starbirths in optical (white and pink), and a selection of current star-forming regions in mm/submm. Inset: ALMA's first mm/submm test views. Credit: ALMA web page,(NRAO/AUI/NSF); ALMA (ESO/NAOJ/NRAO); HST (NASA, ESA y B. Whitmore [STScI]); J. Hibbard (NRAO/AUI/NSF); y NOAO/AURA/NSF.

1.6   Cosmological simulations

Over the past decades the computational power brought to bear in cosmological simulations has been significantly improved, allowing for the possibility of such simulations to assist in the interpretation of cosmological observations (Somerville & Davé review 2015). In particular, there has been an extraordinary progress in simulating the formation of structures, most of them under the current paradigm of the cold dark matter (CDM) model (e.g. Springel et al. (2005), Klypin, Trujillo-Gomez & Primack (2011)). The current generation of cosmological simulations would not be possible without the fast development of N-body simulations (e.g. Aarseth (1963)) starting decades ago. Consequently, with better computational facilities and techniques, the resolution of these simulations has increased, with the CDM model becoming the paradigm of this new understanding.

The tools and methods for cosmological simulations are principally gravity solvers or N-body codes, which determine the force on each mass element by solving the Poisson equation, with the gravitational field sourced by the density distribution of the large-scale structure (Dehnen & Read, 2011). The applied N-body methods may be particle-based, mesh-based or a mixture, as for example in tree codes. These methods model the interactions of DM particles. But to model the visible component of the universe requires modelling gas physics, i.e. solving the equations of hydrodynamics and evolving them concurrently with the chosen gravity solver. Most hydro-codes are based on solving the Euler equations (e.g. SPH code). Another important issue to model galaxy formation is the implementation of thermal evolution. Baryons and dark matter interact in different ways, with baryons able to dissipate their energy via radiative processes. Thus radiative cooling and photo-ionization heating are implemented in essentially all codes. Also, the chemical evolution, i.e. the enrichment of the gas with heavy elements, is often implemented in these hydro-codes.

Modern N-body simulations today reach up to 10^{11} particles, increasing the size of the simulations (Alimi et al., 2012). Furthermore, they include models of astrophysical processes such as cooling of interestellar gas and star formation.

1.6.1   Hydrodynamical simulations

To model the formation of substructures, it is common to use numerical hydrodynamical techniques, so that the equations of gravity, hydrodynamics, and thermodynamics are concurrently solved for particles and/or grid cells representing dark matter, gas, and stars. The simulations of the EAGLE[6] project (Schaye et al., 2015) are a suite of hydrodynamical simulations that follow the formation of galaxies and supermassive black holes in cosmologically representative volumes of a standard ΛCDM universe. Using hydrodynamical codes makes it feasible to obtain predictions of the dark matter, gas, stellar and metallicity densities, as seen in the simulations of the *Illustris project* (Vogelsberger et al., 2014a). Furthermore, the structure and kinematics of galaxies can be studied with great detail (see figs. 1.8,1.7). However, there are

---

[6]EAGLE: Virgo Consortiums Evolution and Assembly of GaLaxies and their Environments project.

still some limitations in these kinds of simulations due to the inability to resolve certain physical processes (at small scales) such as star formation (Sawala et al., 2011), black hole growth and feedback processes. These effects must be included using sub-grid recipes that rely on simple prescriptions and parametrisations.
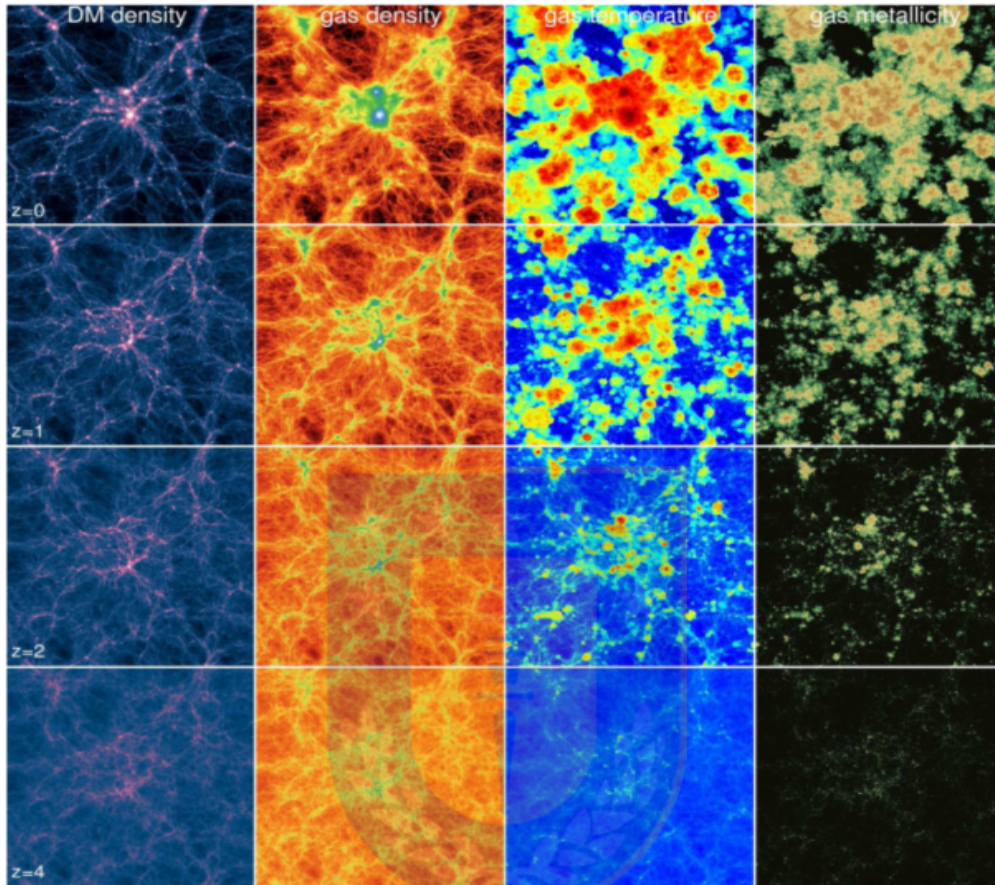
Figure 1.7: Visualization of quantities computed by hydrodynamical simulations (Illustris project), such as the dark matter density, gas density, gas temperature, and gas metallicity at different cosmic times. The slice shown has a projected thickness of 21.3 cMpc and shows the whole Illustris simulation box which is 106.5 cMpc on a side, Vogelsberger et al. (2014b).

1.6.2 Zoom-in simulations

Cosmological codes are able to perform massive galaxy formation simulations containing millions of galaxies (Springel et al., 2005). But it is also possible to perform studies of specific regions of these big simulations. A useful technique is that of *zoom-in* simulations, in which a sub-volume within a cosmologically representative region is evolved at much higher resolution (thus, the spatial resolution in the interesting subvolume can be set at a higher level). The

surrounding regions of coarser resolution provide the tidal field from the large-scale structure. (e.g. Navarro & White, 1994; Tormen, Bouchet & White, 1997). In this method at the end of the whole simulation, a halo or a region of interest is selected, and its particles are tracked back to the original initial conditions to define the zoom region, wherein particles within the zoom region are sampled to finer resolution in new (re)simulations. Therefore the procedure can be described in different steps as *i)* run the low resolution simulation ('the box'), *ii)* identify interesting objects [7] in the box at $z = 0$, *iii)* create new multi-level initial conditions with increased resolution in the interesting volume, *iv)* run the new zoom-in simulation including dark matter only or with baryons. Thus, the simulation of specific regions can be useful to analyse physical processes in more detail.

In this thesis we carry out our analysis of galactic dark matter halos, selected from simulations performed using this technique by Warnick & Knebe (2006). Particularly we analyse eight dark matter galaxy clusters, selected and (re)simulated from a large cosmological simulation.

1.7   Thesis motivation

In the ΛCDM cosmological model, as we have discussed earlier, galaxies and galaxy clusters form through gravitational collapse in the hierarchical structure formation scenario. Dark matter halos first form as small objects and then grow more massive over time. Taking into account that galaxies reside in these DM halos, this model predicts that massive galaxies, galaxy groups and galaxy clusters were built from small galaxies that collided and merged, resulting in these complex structures that we see today. In this context, there is an environmental dependency on the formation and evolution of galaxies, as is evidenced by the changes in their morphology and internal processes, e.g. their star formation. Galaxies evolving in dense environments such as groups and/or clusters as well in the field are affected in different ways. In dense environments they are more susceptible to suffer interactions with other galaxy members, and with the gravitational potential of the group/cluster, leading to effects such as mergers,

---

[7] To identify regions or halos of interest in cosmological simulations it is common to use halo finders (Knebe et al., 2013), which using different techniques are able to identify overdensities in simulations.
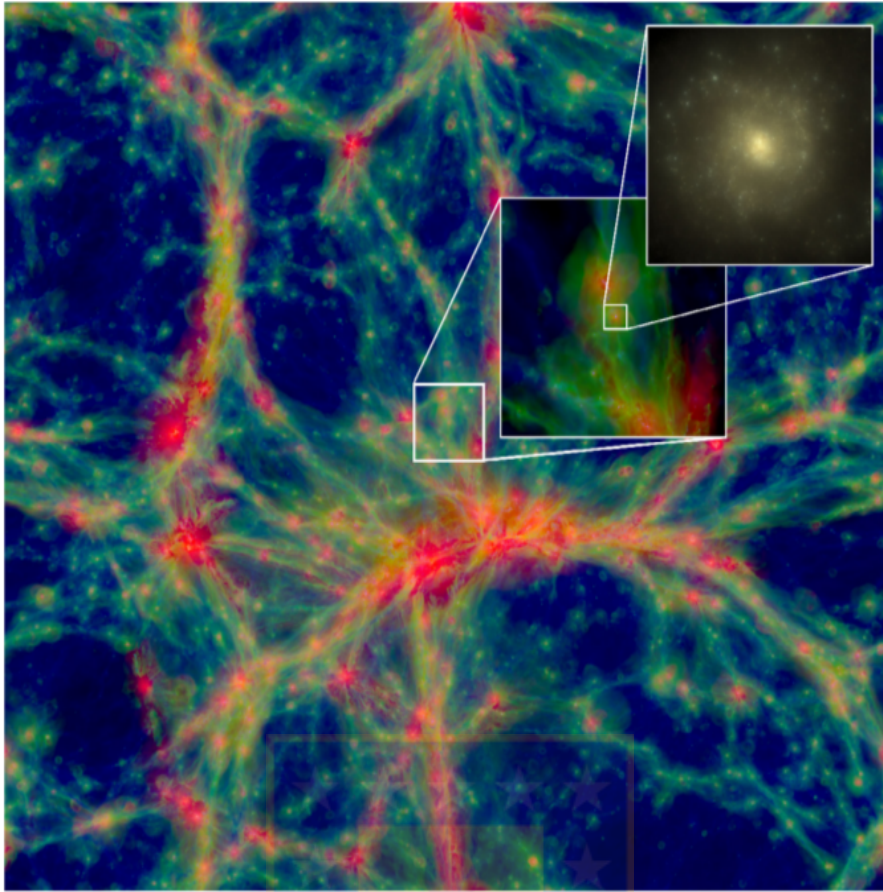
Figure 1.8: Figure of a $100 \times 100 \times 20$ cMpc slice through the EAGLE simulation, illustrating the dynamic range obtained with the state-of-the-art of hydrodynamical cosmological simulations. Inset, a zoom of an individual galaxy with stellar mass $3 \times 10^{10} M\odot$ (Schaye et al., 2015).

harassment, tidal stripping, and ram-pressure stripping. Furthermore, from many studies we know now that a large fraction of galaxies are being accreted into clusters while they belong to a group. Thus before becoming members of the cluster, galaxies are affected by this less dense environment, giving rise to galaxy pre-processing. Consequently, once the group interacts with the intracluster medium, galaxies are affected additionally by the group/cluster interaction (post-processing).

With the advances in cosmological simulations, it is possible to have a wider perspective on structure formation and its evolution at large scales, as well as the evolution of specific regions such as individual galaxies, groups and clusters. Furthermore it is also possible to observe the physical processes in galaxies triggered by the environment in which they are evolving. Many studies (both observational and using simulations) focus on the study of the consequences of the

group and/or cluster environment in the evolution of galaxies. In this context, the aim of this Master's thesis is to perform a study of the consequences of cluster and group environments for the evolution of galactic dark matter halos using high-resolution, N-body cosmological simulations. Thus we aim to address,

i. How does the evolution of a dark matter halo proceed while within a host halo?

ii. How does the mass loss of dark matter halos (members of groups) proceed, and what is the importance of the group and the cluster environment?

iii. What are the main parameters controlling the mass loss?

iv. What causes some group member halos to escape (in some moment of their evolution) from the groups, while others survive?

v. What are the properties of halos that escape from groups?

In order to address these questions, this thesis focusses on studying the effect of the group and cluster environment (simultaneously) on the evolution of a large set of DM halos. We follow the evolution of individual group members, identify what happens to them, what controls the outcome and find out which physical parameters are most important in controlling their evolution. Thus, this study contributes a little more in our understanding of galaxy evolution, and the evolution of dark matter halos in which they are embedded, and how this evolution could be important for the galaxy itself.

Chapter 2

Data and Method

2.1 Simulations

To carry out our analysis of the evolution of DM halos, we use the output data from eight zoom-in simulations performed by Warnick & Knebe (2006). These simulations are based on a suite of nine cosmological N-body simulations, where eight of them were carried out using the publicly available adaptive mesh refinement code MLAPM[1] (Knebe, Green & Binney, 2001).

This suite of simulations is focussed on the formation and evolution of a sample of galaxy and cluster mass dark matter halos containing on the order of one million particles with mass resolution of $1.6 \times 10^8 h^{-1} M\odot$ and spatial resolution of $\sim 2h^{-1}kpc$. These simulations were initially run using independent initial conditions in the standard ΛCDM cosmology at redshift $z = 45$ with cosmological parameters: $\Omega_0 = 0.3, \Omega_\Lambda = 0.7, \Omega_b = 0.04, h = 0.7$ and $\sigma_8 = 0.9$. Here, 512^3 particles were placed in a box of side length $64h^{-1}$ Mpc, giving a mass resolution of $m_p = 1.6 \times 10^8 h^{-1} M\odot$. These simulations were evolved until $z = 0$ and, at this redshift, eight clusters from the simulations were selected with masses in the range $1 - 3 \times 10^{14} h^{-1}$ and other properties as described in Table 2.1.

---

[1] **MLAPM** (multi level adaptive particle mesh) code written in C that is designed to simulate structure formation with collisionless matter. One of the novelties with this code is the way arbitrarily shaped refinements are more efficiently navigated in computer memory, also allowing high-resolution simulations including millions of particles in competitive times.

Host	Mvir	Rvir	λ	V_{max}	R_{max}	$\sigma_{v,host}$	T	age	z_{form}	$\langle\frac{\Delta M}{\Delta tM}\rangle$	$\sigma_{\Delta M/M}$
c1	2.9	1355	0.0157	1141	346	1161	0.365	7.9	1.052	0.128	0.125
c2	1.4	1067	0.0091	909	338	933	0.388	6.9	0.805	0.122	0.156
c3	1.1	973	0.0124	928	236	831	0.265	6.9	0.805	0.100	0.117
c4	1.4	1061	0.0402	922	165	916	0.639	6.6	0.750	0.127	0.207
c5	1.2	1008	0.0093	841	187	848	0.909	6.0	0.643	0.129	0.141
c6	1.4	1065	0.0359	870	216	886	0.073	5.5	0.567	0.147	0.153
c7	2.9	1347	0.0317	1089	508	1182	0.531	4.6	0.443	0.844	1.068
c8	3.1	1379	0.0231	1053	859	1091	0.587	2.8	0.237	0.250	0.225

Table 2.1: Properties of the eight cluster halos (Warnick et al. 2006). Masses are measured in $10^{14}h^{-1}$ $M\odot$, velocities in Km/s, distances in h^{-1} Kpc and the age in Gyr. Here M_{vir} = virial mass, R_{vir} = virial radius, λ = spin parameter, V_{max} = maximum of the rotation curve, R_{max} = position of the maximum, $\sigma_{v,host}$ = velocity dispersion of the host, T = triaxiality parameter, z_{form} = corresponding redshift formation, $\langle\frac{\Delta M}{\Delta tM}\rangle$ = mean rate of relative mass change and $\sigma_{\Delta M/M}$ = dispersion of relative mass change.

The set of eight cluster-sized (host) halos were re-simulated also using MLAPM code (Knebe, Gill & Gibson, 2004). As the resolution is higher in these (re)simulations, this set of simulations has the required resolution to accurately follow the formation and evolution of subhaloes within their hosts. Furthermore, the force and mass resolution is enough to resolve substructures within the virial radius of the host halos.
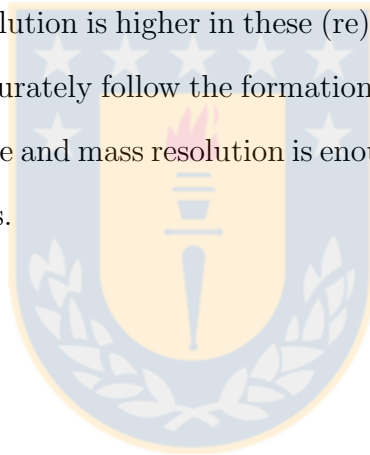
2.2   Halo finder

The identification of the host halos and subhalos, is done using MLAPM's open-source halo finder, AHF (Gill, Knebe & Gibson, 2004). This halo finder uses a numerical technique that is based upon the N-body code MLAPM, and has the same accuracy as the N-body code itself. In general, a halo finder localizes gravitationally bound objects. As halos are centred around local overdensity peaks, they are found using the spatial information provided by the particle distribution, finding local overdensity peaks in the cosmological simulations. To have an idea of exactly how this halo finder works, it is important to have an insight into the mode of operation of the MLAPM (multi level adaptive particle mesh) code first.

2.2.1 MLAPM operating method

MLAPM is a pure grid-based code and uses a recursively refined Cartesian grid to solve the Poisson equation for the potential, rather than obtaining the potential from the Green's function. As the code starts with this Cartesian grid and recursively refines cells (on each consecutive refinement the cells are half the size of the cell in the previous step), using a cell-dependent refinement criterion, such a subgrid can have an arbitrary shape. In high density regions the code places a higher resolution grid in a recursive manner that freely adapts to the actual particle distribution. The adaptive refinement meshes of MLAPM therefore follow the density distribution by construction, thus the grid structure surrounds the subhalos (satellites) as they manifest themselves as overdensities in the underlying background field (as mentioned in Knebe et al. 2004). An example of this is shown in Figure 2.1. The graph shows a slice of a ΛCDM simulation, where the left panel is showing the actual particle distribution, while in the right panel the adaptive meshes invoked by MLAPM are indicated.
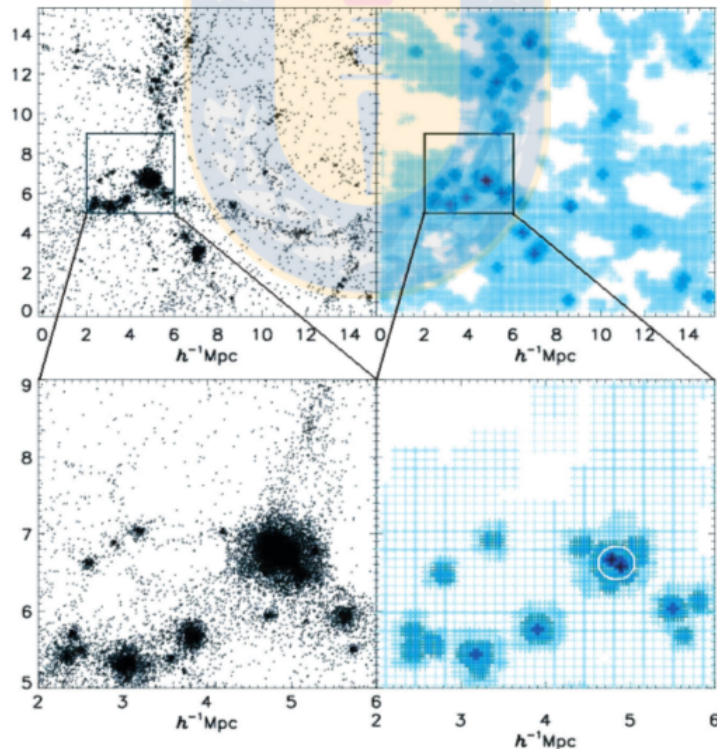
Figure 2.1: Figure showing how MLAPM works. The upper panels show a sample of a ΛCDM simulation. In the left panels the particle positions are plotted and in the right panels the adaptive grid points used to solve the equations of motion are indicated. In the bottom panels a zoom of the specific regions is shown, the white circle indicates the ability of MLAPM's grid to locate substructure (as discussed in Knebe, Gill & Gibson, 2004).

2.2.2   AHF halo finder

AHF uses the adaptive grid of the MLAPM code to locate DM halos, building a register of positions of the peaks in the density field from this grid invoked by MLAPM, to build a list of potential centres. To do this, the algorithm restructures the hierarchy of nested isolated grids into a "grid tree" and the densest cell at the end of these "branches" denotes the centre of a prospective DM halo. Making the assumption that these peaks in the grid (the potential centres) are the centres of halos, the algorithm steps out in radial bins until the overdensity reaches a limit set by the background cosmological model. Then, it is possible to define some properties such as the virial radius and provide a list of particles associated with the dark matter halo (as is pointed out in Gill et al.2004). Once all the gravitationally unbound particles are removed (using the potential centre again and applying a velocity criterion to the particles inside the halo), the halo finder provides us with a table containing the positions of the halos, but also other properties, such as virial radius, virial mass, velocity dispersion and density profile for each DM halo at every snapshot.

An advantage of this halo finder is the level of accuracy, as the N-body code itself is free of any bias and discrepancies between simulation data and halo finding precision. The finder algorithm is fully recursive in identifying automatically halos and subhalos. But the disadvantages of halos finders (in general) are the lack of perfection in obtaining the halo properties, the disappearances of halos between snapshots in dense environments, mass and edge determination, etc. Halo finders, and the halo model in general, are a convenient way to treat a large, virialised collection of dark matter particles, but they are always an approximation to the true underlying dark matter distribution.

Our sample of eight cluster halos and subhalos is identified using this halo finder. As the simulations have the required resolution to follow the evolution of subhalos within hosts (down to a minimum halo mass limit set by the minimum number of halo particles required to define a halo, which is set at 20), we are able to do our current analysis using the output data containing the necessary information for each dark matter halo.

2.3 Quantities and definitions

With the data provided by the halo finder for each of the eight cluster-sized halos and for each of their DM subhalos at every snapshot, we identified the target sample to study: group halos and group-member halos using a simple but effective criterion. To do the initial identification (at the beginning of each simulation) we use an algorithm, written in FORTRAN, to compare the positions, velocities and masses for each halo in their respective clusters. Our code implements this criterion by calculating several variables for each of them, in order to do a comparison.

The first quantity calculated is the relative distance (r) between two DM halos:

$$r = \sqrt{(x_1 - x_2)^2 + (y_1 - y_2)^2 + (z_1 - z_2)^2}. \tag{2.1}$$

In this equation x_1, y_1, z_1 denotes the position of the "test halo" and x_2, y_2, z_2 denotes the position of the halo with which we are doing the comparison.

$$V_{rel} = \sqrt{(v_{x1} - v_{x2})^2 + (v_{y1} - v_{y2})^2 + (v_{z1} - v_{z2})^2}. \tag{2.2}$$

Here V_{rel} is the relative velocity, and again v_{x1}, v_{y1}, v_{z1} are the velocities for the "test halo" and v_{x2}, v_{y2}, v_{z2} are the velocities of the other halo. Also, to ensure that we are considering bound objects, we calculate the escape velocity V_{esc}.

For those halos that are inside of R_{vir} of the candidate host, the escape velocity in a NFW profile is given by

$$V_{esc} = \sqrt{\frac{2GM_{vir}}{R_{vir}}} \sqrt{g_c ln(1 + cs) - ln(1 + c) + 1} \qquad if \;\; r < R_{vir} \tag{2.3}$$

where M_{vir} is the virial mass of the candidate host halo, R_{vir} its virial radius, G is the gravitational constant, and c the concentration parameter. Here g_c denotes

$$g_c = \frac{1}{ln(1+c) - c/(1+c)} \tag{2.4}$$

and,

$$s = \frac{r}{R_{vir}}. \tag{2.5}$$

The escape velocity associated to subhalos located at a distance larger than the virial radius of the candidate host halo is

$$V_{esc} = \sqrt{\frac{2GM_{vir}}{r}} \qquad\qquad if \ \ r > R_{vir}. \tag{2.6}$$

With these parameters, we select the halos hosting subhalos in each cluster (at the first snapshot of the simulations), but excluding the most massive halos, as they include most of the halos as their members, causing our selection sample to be reduced. Therefore we ignore the halos with masses larger than $\sim 10^{13} M\odot$ and with radius larger than $400 Kpc$.

In agreement with these conditions, we define a **_group halo_**[2] as a DM halo that is hosting (lower mass) subhalos within. And **_group-members_** as halos whose center (or relative distance) is inside $2R_{vir}$ of a host halo, also considering that the relative velocity between them is less than the escape velocity, i.e. bound subhaloes. Figure 2.2 shows a simple diagram about the classifications.

We stress out that, through this analysis, we use the terminology of *group* to distinguish between the halos that contain no subhalos (referred to as group-members) and the clusters.

2.3.1   Survivor, escaper and destroyed group-member halos

After identifying DM halos as groups and group-member halos, Figure 2.3 shows how we classify the group-member halos according to their subsequent behaviour while they are evolving in a

---

[2]The halos were specifically selected to investigate the evolution of subhalos in host halos (groups). But, in the general context of "group definitions", in this study we classify them as an aggregation of halos comprising at least two bound members, i.e. two bound DM matter halos is a group.
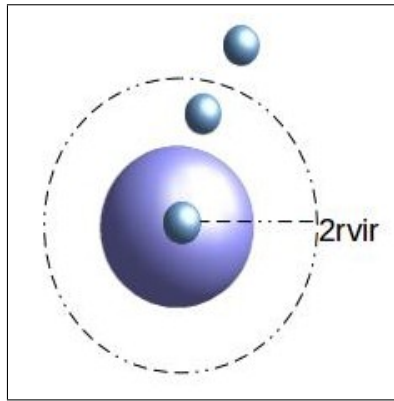
Figure 2.2: Diagram showing the DM halo selection at the beginning of the simulations, according to a mass, velocity and radius criterion. The biggest bubbles denote a group halo, and the dashed line around it denotes a distance of $2R_{vir}$ from its center. The small bubbles inside this distance are denoting group-member halos. The bubble located outside the dashed line demonstrates a DM halo that does not comply with our criterion, i.e. it is not a group or a group-member.

host. In order to differentiate the halo behaviours, we define:

- *Survivor group-member halos:* halos that during their evolution in the simulation remain as a group-member, i.e., at every snapshot of the simulation, their relative distance from the center of their group is less than $2R_{vir}$.

- *Escaper group-member halos:* halos that at some point of their evolution reach a distance greater than $2R_{vir}$ with respect to their group, i.e., they escape from it. In the simulations, some DM halos reach a mass below the mass resolution limit, but when a group-member halo reaches this limit while already being outside this distance we classify them as "escapers" (as we are interested in them only until the moment in which they escape).

- *Destroyed group-member halos:* As we mentioned before, both group-member and group halos during their evolution may lose mass and eventually reach a mass which lies below the mass resolution limit of the simulation ($1 \times 10^{10} M\odot$). Some group-member halos reach this limit when they are inside of their host. In our analysis we do not consider these halos, which somewhat reduces our sample size.
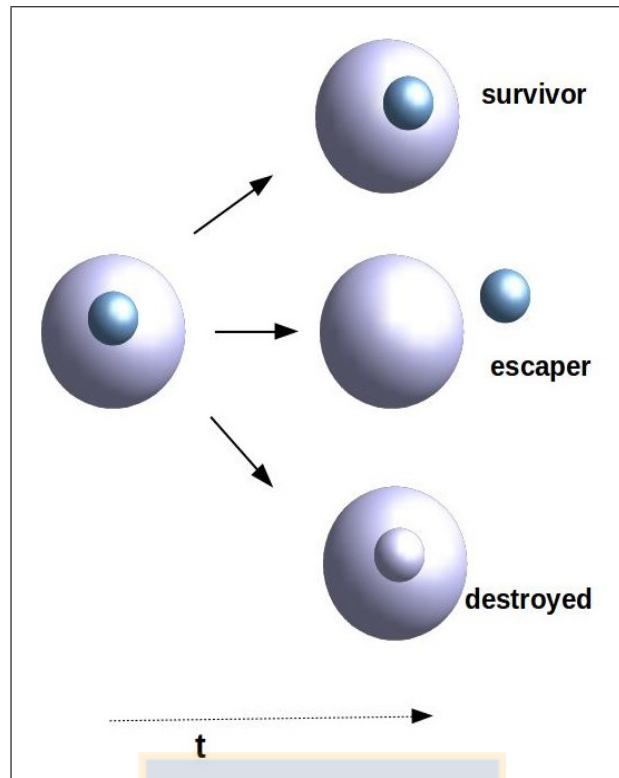
Figure 2.3: Diagram showing the group-member DM halos classification. The different possible behaviours of the group-member halos (small bubbles) while they are evolving inside their host halos (large bubbles) are shown in the three options on the right hand side of the diagram. *Top:* a group-member halo surviving inside its host. *Middle:* a group-member halo escaping from its host. *Bottom:* a group-member halo destroyed within its host, i.e. its mass went below the mass resolution limit.

2.3.2   Orbit classification: sinker and orbiter group-member halos

In addition to the final state of the group-member halos discussed above, we find it necessary to distinguish the kind of orbital behaviour that the group-member halos exhibit inside their host. To do this, we use a straightforward criterion: using a simple moving average method (i.e. we create a series of averages of different subsets of the full data set, with their respective standard deviation at every point), we smooth the orbit in order to eliminate the noise of the curve.

Once the orbit is smoothed, we identify a ***sinker*** group-member as a halo whose averaged distance to the centre of its host/group is at least one standard deviation below $0.2R_{vir}$ for most of the time of their evolution in the simulations, typically $> 50\%$ of the total time. The standard deviation of the smoothed orbit is calculated with the original orbit. This means they are sinking very close to the centre of the host, as we can see in Figure 2.4. An example of this

criterion is shown in this figure. The teal colour line denotes the original orbit and the yellow line denotes the smoothed orbit. The dashed blue line in this plot shows the distance limit imposed.

To classify a member halo as an ***orbiter***, we just define them as those halos that do not have the behaviour described before, i.e. they are not sinkers. For example, The total number of survivor group-members that we identified as sinkers or orbiters is 44 and 101 respectively (refer to Fig. 3.19).
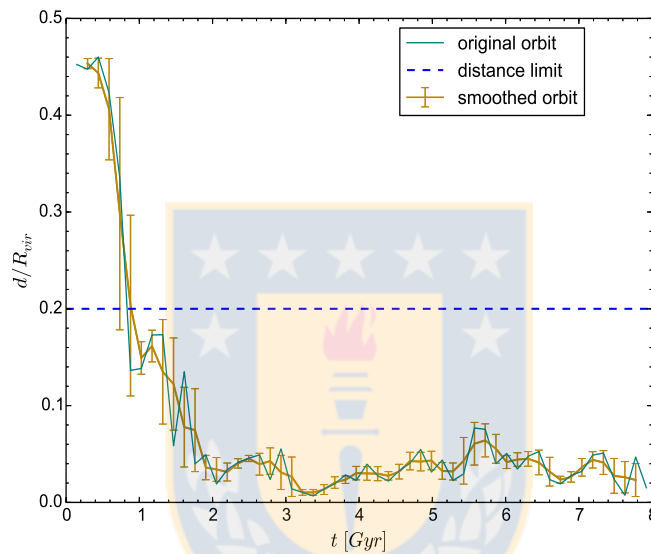
Figure 2.4: Example of our criterion to classify sinker and orbiter group-member halos. The teal colour line denotes the original curve for the halo's orbit (scaled to the R_{vir} of the host). The gold colour line denotes the smoothed orbit obtained by using a moving average plus the standard deviation. The dashed blue line shows the limit imposed on the orbital distance for a halo to qualify as a sinker.

Chapter 3

Results

In the ΛCDM framework, tidal forces are a common phenomenon, playing an important role in the formation and evolution of dark matter halos. The interplay of gravitational effects and the subsequent evolution of these halos are closely related. As structure grows, some galaxies join massive systems, therefore experiencing a variety of environments during their lifetimes, and therefore a variety of tidal interactions.

Our analysis, using the classification scheme described in Chapter 2, attempts to find the consequences of these tidal interactions for the group and group-member halos, particularly in relation to mass loss and orbital characteristics.

3.1   Initial general properties

The selected sample contains 441 group-member halos in 237 group[1] halos. In the table 3.1 we detail the total number of halos, the number of the target sample, and the number of the sub-classification that we did on the group-member halos in each cluster. From the total number of group-member halos, we identified 145 of those that are "surviving", 122 "escaping", and 172 that are being "destroyed" in their host group.

---

[1]Through this analysis, we use the terminology of *group* to distinguish between the halos that contain no subhalos (referred to as group-members) and the clusters.

Some of the main properties that the group and group-member sample have are shown in Fig.3.1. For example the group masses are in a range of $(10^{10} - 10^{13})M_\odot$, while their radius are a in a range of $30 - 400$kpc. Group halos are initially found at a wide range of distance with respect to the cluster centre, from $\sim$ (0.1 - 7) times the virial radius of the cluster. But the fraction that are initially already inside the cluster's virial radius is quite small ($\sim$ 8 per cent). This makes our identification of group members much more robust. Many of the groups that we consider in our sample typically contain just one group-member halo ($\sim$ 65 per cent). $\sim$17 per cent contain two group-members, and $\sim$ 8 per cent contain three group-members. The most massive groups in our sample contain up to 11 member halos. Regarding to the mass range, a 32 per cent of groups have masses greater than $10^{12}M_\odot$, while the less massive remaining groups correspond to 68 per cent.

cluster	N_{tot}halos	Nhalos	group-member	group	survivor	escaper	destroyed
c1	1632	1626	134	70	27	45	62
c2	987	983	58	33	32	12	14
c3	401	398	35	14	4	19	12
c4	793	787	22*	17	15	4	2
c5	557	554	23	15	11	3	9
c6	452	448	30*	16	11	7	11
c7	769	766	78	41	25	10	43
c8	634	628	61	31	20	22	19
tot	6225	6190	441	237	145	122	172

Table 3.1: Second and third columns with the total number of DM halos on each cluster, and the total number of DM halos not considering those too big ($r_{vir} < 400Kpc$). The number of group-members and group halos on each cluster (forth and fifth). The three last columns are the numbers of the group-members who were identified as "survivor","escaper", and "destroyed" according to our classification. Note, the (*) symbols is denoting a group-member who is not at any category, as its group is destroyed early, i.e., its mass go below the resolution limit.

3.2 Dark matter mass loss

In order to study how the cluster and group environments are affecting the group-member halos (and also the groups themselves), we investigate the mass loss of the DM halos when they are evolving in and around a galaxy cluster.
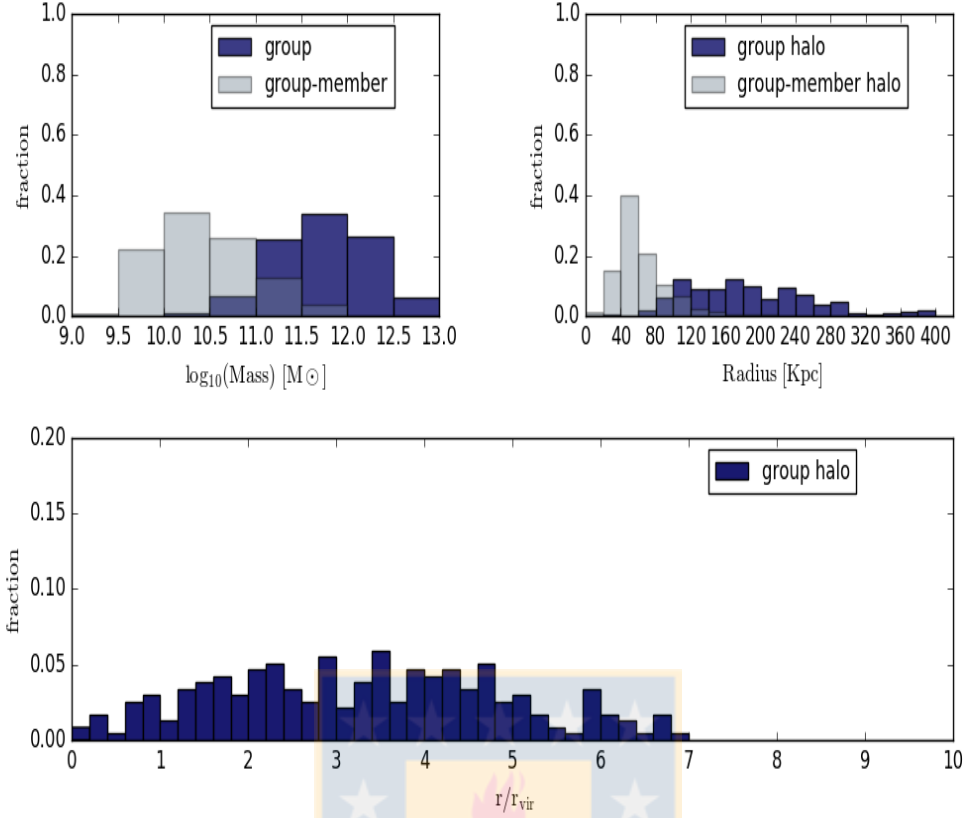
Figure 3.1: General properties for the selected sample. *Top:* Distribution of mass (left panel) and radius (right panel) for group and group-member halos, denoted in gray bars and light gray bars respectively. *Bottom:* Distribution of the initial group locations with respect to the cluster center; distances are scaled to the R_{vir} of the cluster.

3.2.1   Group halos

First, we analyse how much mass is lost and where the group halos are losing mass, especially for those evolving in the outer regions of the cluster and for those entering the inner regions. Figure 3.2 shows the fractional mass loss of the group halos, i.e. We compare the final mass (m_f) at z = 0 with the initial mass (m_i), and we define the fractional mass loss to be $f_{dm} = 1 - m_f/m_i$. DM halos losing a high fraction of their dark matter mass will have $f_{dm} \sim 1$, whereas those that lose little dark matter will have $f_{dm} \sim 0$. We split the sample of group halos into two subsamples: those group halos that always have a cluster-centric distance of greater than $2Rvir$, and those that enter within $0.5Rvir$ at least once. Groups (middle panel)that stay far from the cluster (blue unfilled bars) lose very little mass (the distribution is skewed left), in comparison with groups which interact with the cluster environment (grey filled bars) where the distribution is

much flatter, indicating that many groups lose substantial quantities of mass. This indicates that groups outside the cluster are not interacting with larger structures, leading to significant mass loss (i.e. filaments, and large-scale structures), but when they enter the cluster,the tidal effects experienced there appear to be the most important in causing an enhanced mass loss
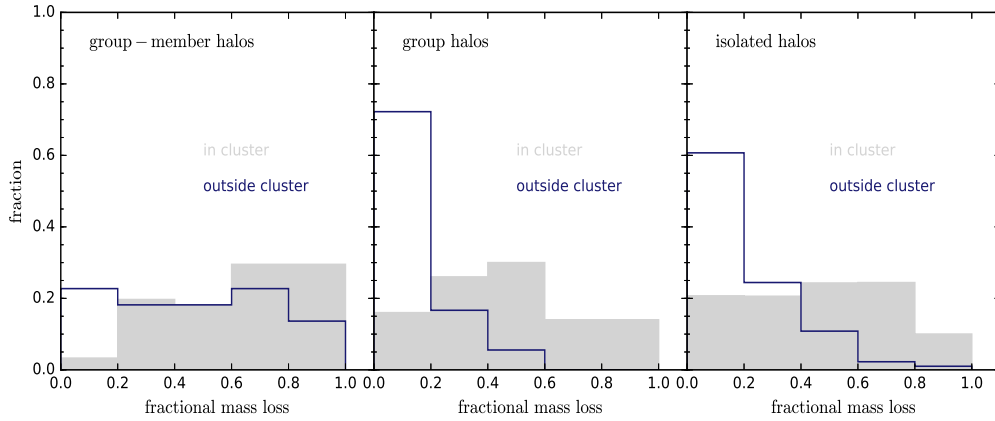
Figure 3.2: Distributions of the fractional mass loss of group-member halos (top panel), group halos (middle panel) and isolated halos (bottom panel). This quantity is measured for halos that are evolving outside the cluster, i.e. $r_c \geq 2r_{vir}$ at all times, where r_c is the halo clustercentric distance (unfilled blue bars), and for those halos for which $r_c \leq 0.5r_{vir}$ at least once during their evolution (filled grey bars).

3.2.2 Group-member halos

When studying the mass loss of the group-members (left panel) we find that the group-members in those groups which remain outside the cluster exhibit mass loss fractions equally distributed from 0 to 1. On the other hand, for those groups which enter the cluster, we preferentially find group-members in bins with higher mass loss, i.e. typically they retain only a small fraction of their mass. Therefore, the broad spread of the histogram for group-members outside the cluster shows that the group environment is already able to cause severe mass loss in some of their member halos, and presumably in the galaxies within those halos.

This picture changes once the groups fall into the cluster and spend sufficient time in the cluster environment. The histogram clearly shows that the halos experience a much stronger mass loss due to the combined effects stemming from the group itself plus the destructive forces from the

cluster. Therefore, inside the cluster, the majority of halos exhibit strong and very strong mass loss, leading to higher fractional mass loss.

Furthermore, if we compare the total fraction of dark matter mass lost with the isolated halos[2] (right panel Fig.3.2), we see that the distribution is quite similar to that of the group-halos (middle panel). Most of the isolated halos evolving outside the cluster lose just a small fraction of their mass, typically less 20 per cent (peak of the unfilled bars), meanwhile those entering the cluster tend to lose more mass (flat distribution of grey filled bars, showing a wide range of mass loss). This is because isolated halos outside the cluster are not surrounded by other structures which could cause strong tidal forces and, as a consequence, strong mass loss. Isolated halos inside the cluster, however, do experience a strong enough tidal effect to strip a larger fraction of their mass. Furthermore, this indicates that the group-member halos do not have a strong effect on their host groups. If this were the case, one would expect that the group halos would lose more mass than the isolated halos, i.e. the differences between the distributions (grey filled bars in the middle and right panels of Fig. 3.2) would be more noticeable. It is clear, however, that the groups have a strong effect on their member halos (top panel).

3.2.3   Mass loss rate

In the previous section we saw how much mass loss occurs, but we have yet to explore *when* this mass loss occurs. Figure 3.3 shows the fractional mass loss for groups ($f_{dm}(t)$) every 1 Gyr after the start of the simulations. Here, the histograms in the right panels show the change on mass of groups. We note that bars distribution for groups outside the cluster (blue unfilled bars) tend to be concentrated in the bins with lower fractional mass loss through the time, i.e. they are losing a little fraction of mass. In contrast, those groups entering the cluster (grey filled bars) tend to move to the bins with a higher mass loss. This suggests that these halos are not losing large amounts of mass while they are in these outer regions, and any such mass loss that affects this subsample of halos takes place on a long timescale. On the other hand, we see that groups that enter clusters, with a pericentre passage of less than $0.5r_{vir}$, experience

---

[2]These are halos that do not host any subhalos throughout their entire evolution in the simulation.

strong tidal effect in cluster which is reflected by their elevated mass loss. Furthermore the rate at which this population of group halos is affected by mass loss is significantly faster than for those groups remaining outside the cluster, as made clear by the more rapid evolution of the histograms in this case from the left of the plot (no mass loss) to the right (significant mass loss).

Moreover, outside the cluster environment the group halos lose almost no mass. Those which do lose mass, are slowly approaching the cluster. Inside the cluster, we detect stronger mass loss of groups, but still we see a significant fraction of unharmed group halos at all times as groups are constantly falling into the cluster environment[3] (especially after 4 Gyr, refer to histogram 3.4 or section 3.4.2). The population of group halos that has fallen into the cluster by any specific time will generally experience stronger mass loss, shifting their location in the histogram to the right. For example inside the cluster, at three Gyr, half of the total fraction of groups have already lost more than 20% of their masses, and through time we see that the fraction of groups losing high percentages of their 'initial' mass is increasing. On the other hand, outside the cluster, most of the groups only lose $\sim 20\%$ of their initial mass (for most of the time), and around six Gyr this percentage of mass lost increase a little bit. This means that groups are not losing much dark matter mass outside the cluster, and it could be due to the fact that in these outer regions, they are not in larger structures that can cause significant mass loss. So when they are entering the cluster they become more affected by the tidal effect of this environment and, as a consequence they are losing more mass (as was also mentioned in section 3.2.1).

---

[3]To clarify, there are very few groups that already are inside the virial radius of the cluster when we start the analysis, i.e., since the first snapshot that we are able to observe the different properties for our cluster sample.
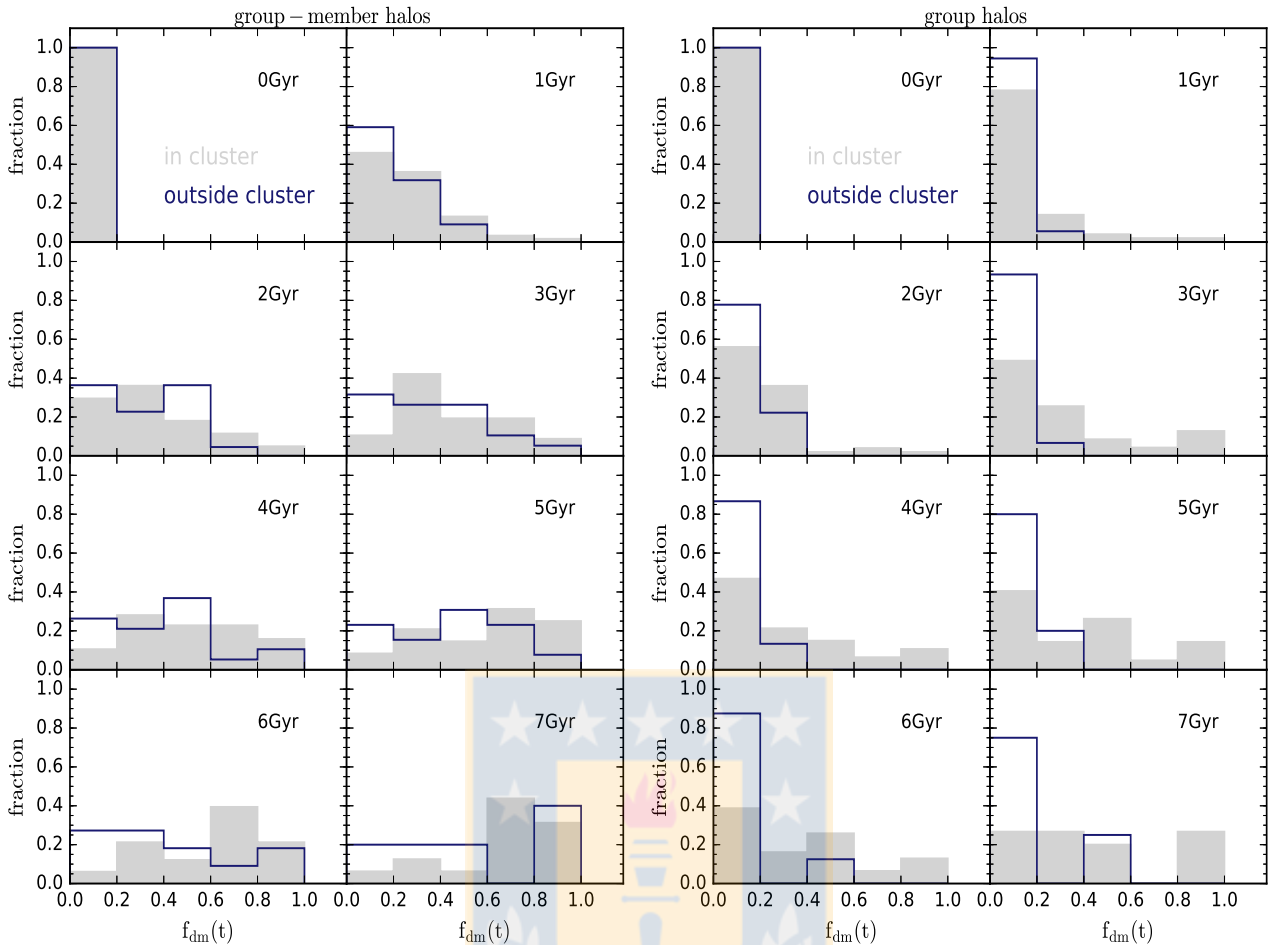
Figure 3.3: Dark matter mass loss evolution for group-member halos (left panels) and group halos (right panels). The filled grey bars denote those halos that enter the cluster (i.e. $r_c \leq 0.5 r_{vir}$ at least once), while the unfilled blue bars denote those halos that remain outside the cluster (i.e. $r_c \geq 2 r_{vir}$ throughout the simulation). The distributions of fractional mass loss ($f_{dm}(t)$) are measured every Gyr, starting from the first snapshot in the simulations (first panel; 0Gyr).

In contrast to the group halos, the mass loss of the individual group-members (left panels) is mainly dependent on the group environment itself (section 3.2.2). Thus, we analyse how their mass loss is proceeding through time. We see in figure 3.3 that the bars distribution is rather similar in both samples and progressively these move to the regions with higher mass lost (particularly those entering in the cluster; grey filled bars). For example at one Gyr, roughly half of the group-members (both in and outside the cluster) have lost more than 20% of their masses. This suggest that the mass loss happens in a continuous way and we note that the fraction of group-members with similar mass loss is similar in the two subsamples. But, the fact that the overall rate of change in the mass loss distributions for the group-member halos

has no dependence on whether the group is inside or outside the cluster is further evidence that the group tides dominate over the cluster tides for all group-members. This changes a little bit at later times when the groups are closer to the cluster centre (see fig. 3.4) and the cluster tides become more important, not only for the group-member halos, but also for for the groups themselves. Therefore, as we noted before, some groups are not protecting much their group-member halos from external cluster tides, even if some of them have sunk to the group centre.
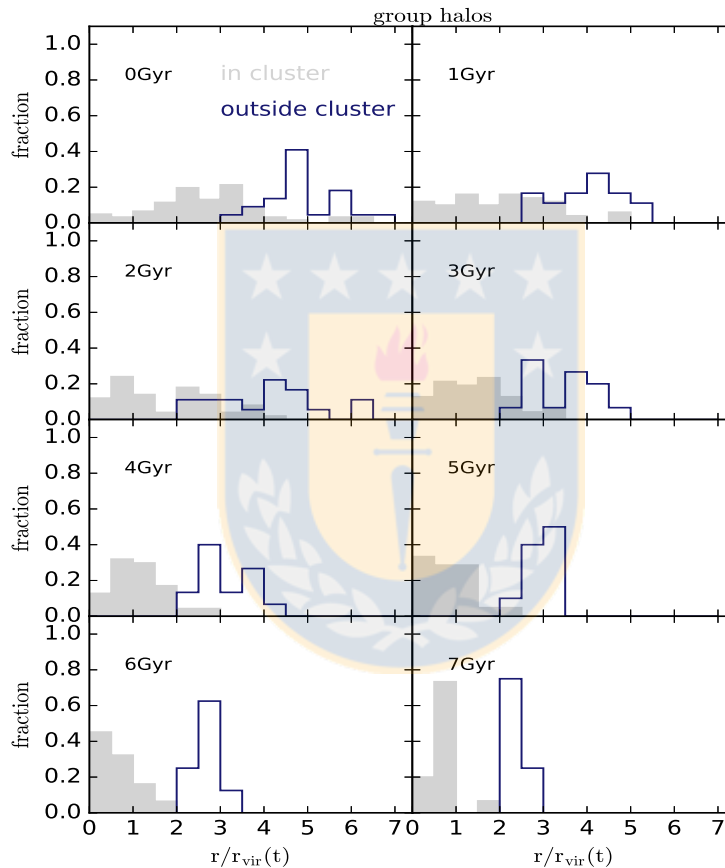
Figure 3.4: Histograms showing how groups change their cluster-centric distance. The distance r is given in units of the virial radius of the cluster r_{vir}. The filled grey bars denote those halos that enter the cluster (i.e. $r_c \leq 0.5 r_{vir}$ at least once), while the unfilled blue bars denote those halos that remain outside the cluster (i.e. $r_c \geq 2 r_{vir}$ throughout the simulation).

3.3   Orbital parameters

The orbital parameters can set the conditions which control their subsequent evolution, for example the evolution of the mass. Taking into account the kind of orbit, we find it is necessary to distinguish two types of orbits (as not all of them have similar behaviour while they are orbiting within their host), so we designate: "sinker" and "orbiter" group-member halos, as described earlier (Chapter 2, section 2.3.2).
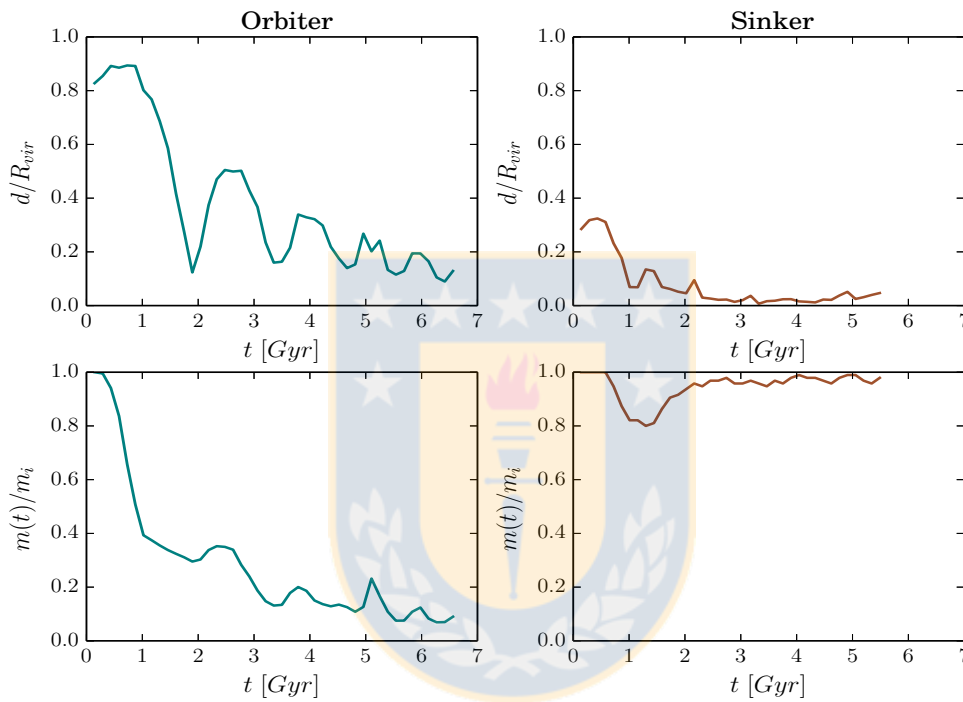
Figure 3.5: Examples of the orbit and mass behaviour for orbiter and sinker group-member halos. *Left panels:* Orbit of the halo, measuring the distance scaled to R_{vir} of the group halo. Here we have classified an orbiter as a halo which is "following a regular orbit", i.e. it is not sinking to the center of its host halo (top; red line). A sinker is a halo sinking very close of the center of the group for most of the duration of the simulation; in particular it has a distance less than $0.2R_{vir}$ with respect to the group halo (bottom; blue line). *Right panels:* We compare how these two cases are losing mass. The red lines are for the the orbiting halo and the blue line for the sinking halo.

3.3.1 Orbiter and Sinker

As described in Chapter 2, we define a *"sinker"* as a group-member halo whose orbit sinks very close into the center of its host group. They evolve inside a distance of less than 0.2 times the virial radius of the group for most of the duration of the simulations. An *"orbiter"* is a group-member halo which has a "regular orbit" i.e. they do not sink to the centre of the host group.

Physically, a sinker halo, being effectively a halo merger, would likely correspond to a galaxy merger, because the smaller dark matter subhalo is close to the center of the larger host halo due to dynamical friction. The close proximity of the two galaxies would likely result in a close interaction, leading to a merger. Interestingly, we also note that when a subhalo is very close to the center of the host halo, it is not necessarily disrupted immediately at all. However, the connection between a halo merger and a galaxy merger is not straightforward and, in this project we limit our analysis to dark matter only simulations. In the future it would be desirable to confirm this by conducting future modelling that includes the baryonic content of galaxies...to understand if real galaxies can sink to the centre of more massive systems, and yet remain as bound entities.

An example of the orbital evolution of the orbiter and sinker classifications is given in Figure 3.5. We see that in these two cases, we have a significantly different behaviour in the mass loss. A sinker tends to lose much less mass than an orbiting halo, as they are less susceptible to the tidal effect and so, seem to be tied to the fate of their host halo (as discussed below).

3.3.2 Mass loss in and out of the cluster, for sinkers vs orbiters

Figure 3.6 shows the fractional mass loss (as defined in section 3.2.1) for these subhalo populations, i.e. orbiters and sinkers. The histograms in the top row are showing the fractional mass loss for sinkers evolving in groups outside (right panel) and inside the cluster (left panel), with "outside" and "inside" defined as before. We see here that in the outer regions of the cluster, sinker halos tend to lose little mass once they have sunk (top right panel). The group-member

halos outside the cluster classified as orbiters (bottom right panel), however, lose more mass as they remain susceptible to group tides in comparison to the sinkers, as these ones are being tied to the fate of their groups. As these group members are outside the cluster, and most groups only contain one group member, the primary source of tidal mass loss must arise from the group halo itself. In the bottom row histograms we observe how the orbiter halos are losing mass (in groups outside and inside the cluster). Here we note that the tides of the cluster cause similar mass loss for orbiters and sinkers alike (top left and bottom left panels), indicating the additional effect of the cluster tides once groups and their members are falling into this environment. But, we note that the change between the sample in and outside the cluster is only significant for sinkers, as inside the cluster they are more exposed to additional tides and so, groups are not protecting their members for external tides.
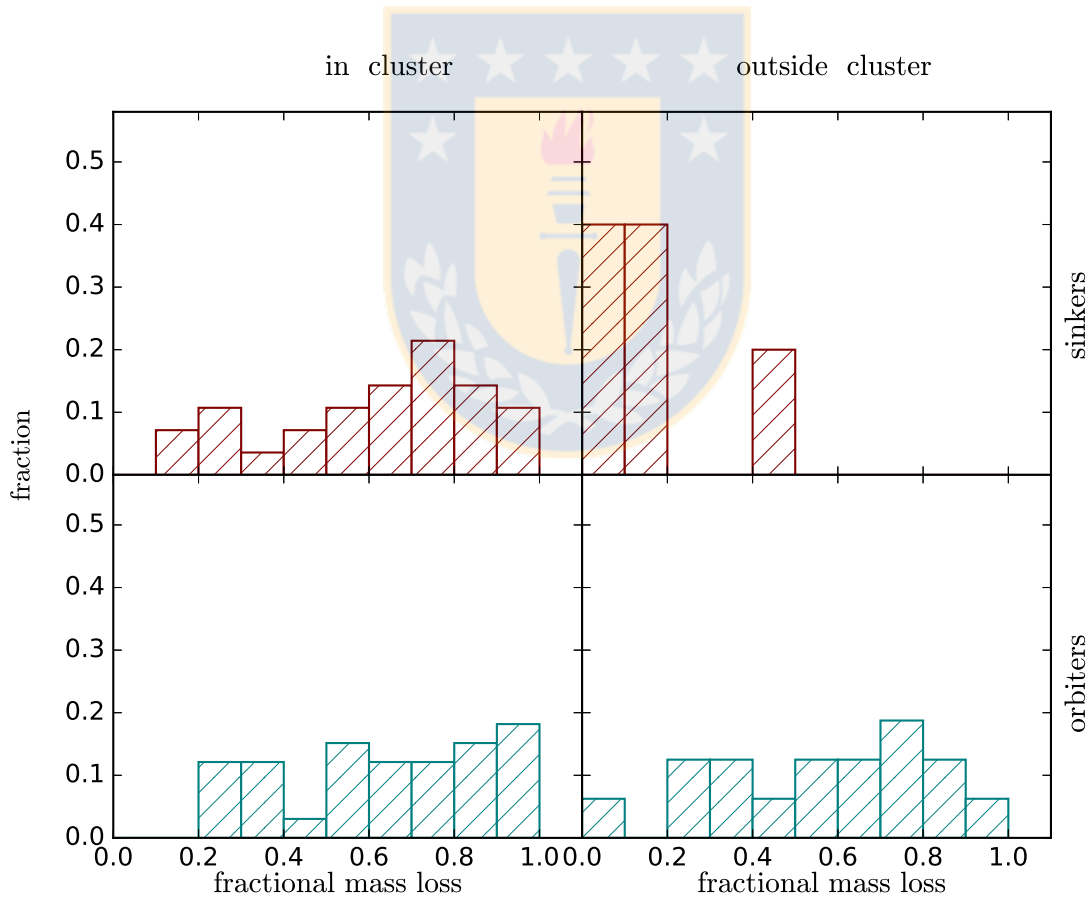

Figure 3.6: Histograms of the fraction of group-member halos (y-axis) as a function of their fractional mass loss (x-axis). In the top row, red bars show sinker halos in groups evolving inside and outside the cluster. In the bottom row, blue bars show orbiter halos in groups, again split between groups that are inside or outside the cluster.

3.3.3   Dynamical friction

Figure 3.7 shows the initial mass ratio m_{gm}/m_g between the group-member halo and the group (mass of the group member (m_{gm}) divided by the mass of the group (m_g) at the beginning of the simulation), for *sinkers* and *orbiters*. Again we compare the location in the cluster where they are evolving (inside or outside the cluster). What we see is that sinkers tend to be the more massive group members, compared to their group mass (both in and outside the cluster). As this ratio is larger for these halos, this supports the contention that they are sinking in their group due to the effect of dynamical friction, which is more efficient in dragging them to the central parts of their host, in comparison with the orbiter halos whose initial mass ratio for most of them is smaller than 0.1. These sinker halos must lose energy/momentum and slow down while they are falling into the central regions of their host halos.

Going further with the dynamical friction effect on group-member halos, the time-scale for the Sinker and Orbiter halos was compared. This time-scale was estimated using the Chandrasekhars formula (Taylor & Babul, 2004), which points out the rate at which the satellite loses its angular momentum. In the case of a circular orbit, the time-scale is given by,

$$t_{scale} = k \frac{M_h/M_s}{ln(M_h/M_s)} \frac{P_{vir}}{2\pi} \tag{3.1}$$

where M_h is the mass of the main halo, M_s is the initial mass of the subhalo (satellite) and k is a constant. For an orbit in a singular isothermal sphere, k = 1.17 (Binney & Tremaine 1987), and P_{vir} is given by the equation,

$$P_{vir} = \frac{2\pi r_{vir}}{V_{c,vir}} \tag{3.2}$$

Here $V_{c,vir} = V_{infall} = \left(\frac{GM_{vir}}{r_{vir}}\right)^{1/2}$ is the orbital velocity for the subhalo when it 'merges'. For non-circular orbits in an isothermal halo, $t_{scale}(\epsilon) \simeq t_{scale}\epsilon^{\alpha}$ (Lacey & Cole 1993). The parameter ϵ is the initial circularity of the satellite's orbit which depends on the eccentricity as $\epsilon = \sqrt{1 - e^2}$ (Wetzel 2011), and $\alpha = 0.78$.
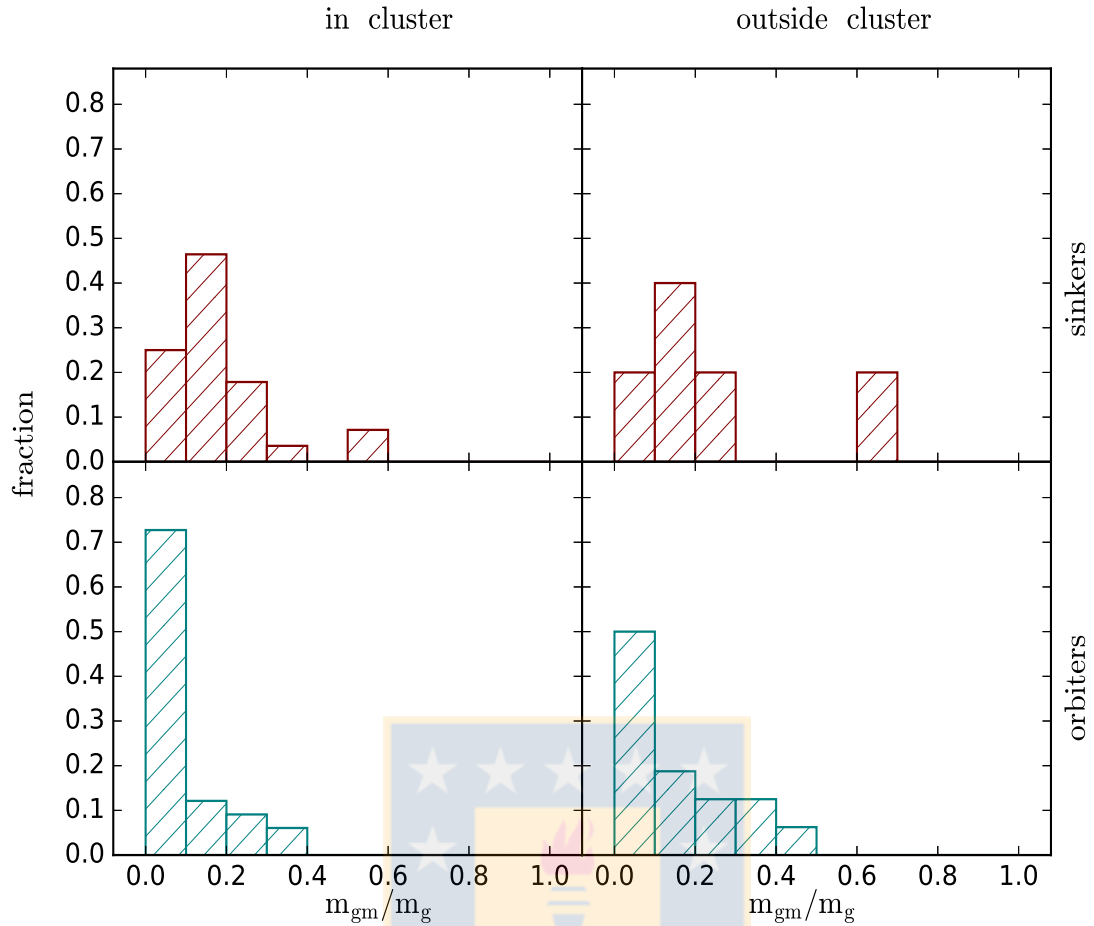
Figure 3.7: Distribution of the initial mass ratio m_{gm}/m_g between the group-member halos and their groups (mass of the group member (m_{gm}) divided by the mass of the group (m_g) at the beginning of the simulation). Top row histograms show this ratio for sinker halos, and orbiter halos are shown in the bottom row histograms. Columns show the location were these halos are evolving, inside and outside the cluster.

Histograms (Fig.3.8) show the distribution of this time-scale depending of the circularity (t_{scale}) for Sinkers (red bars) and Orbiters (blue bars). This is shown again for those evolving in and outside the cluster. We see that most of sinker halos are concentrated in the bars having a less time-scale (most of them between $\sim 3.9-10$ Gyr), meanwhile the orbiter's bars are more spread in the range of this time, i.e., having larger time-scale. Thus, we see that, longer time-scales tend to be for orbiters, and smaller ones tend to be for sinkers. In addition to what was showed previously (higher mass ratio m_{gm}/m_g between the group-member halo and its group for sinker members), this result (taking into account that it is an approximation) gives us an idea why dynamical friction effect is more effective on sinkers, as they will reach the most internal region earlier in comparison with the other ones orbiting (not sinking). In relation about the main

factors controlling the mass loss, the kind of orbit of group-members is an important constraint of how much mass the group-member halos lose.
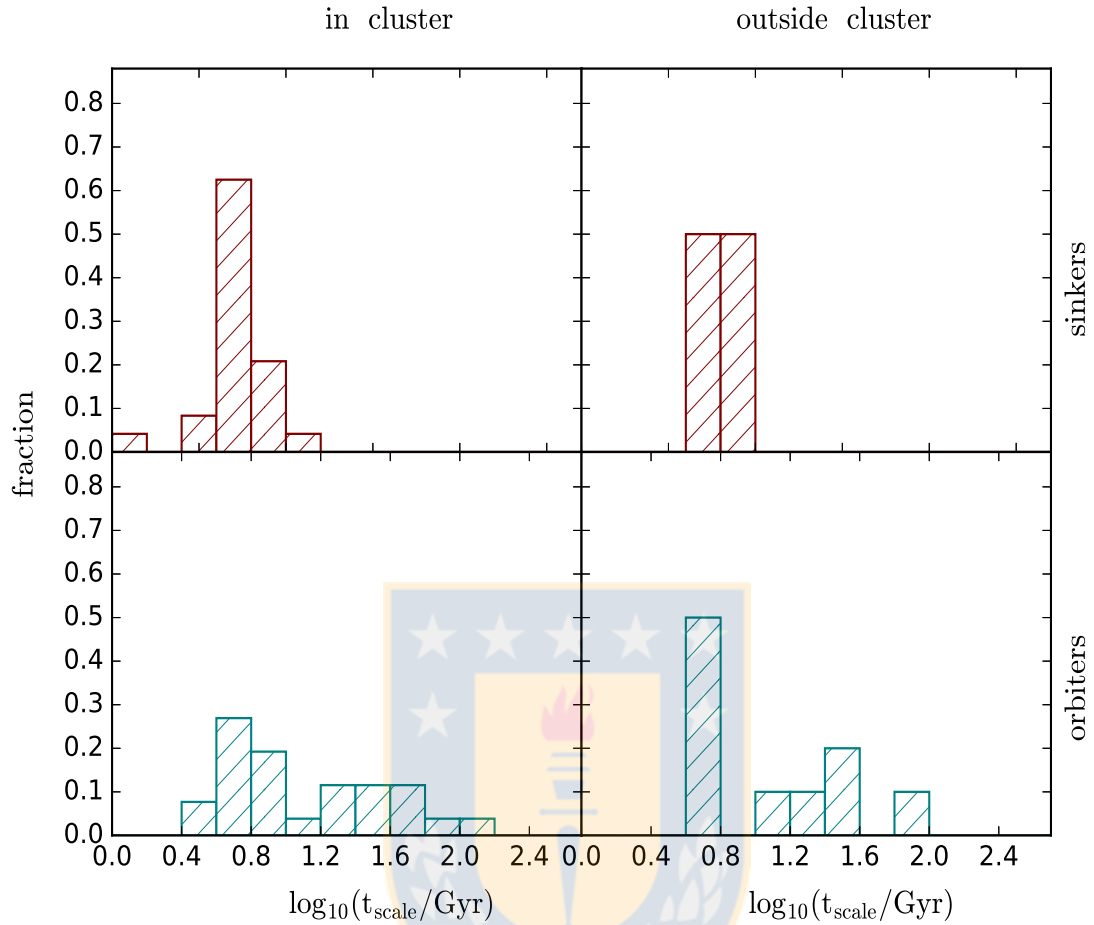
Figure 3.8: Time-scale distributions for group-member halos. For sinkers on red bars (top panels) and for orbiters on blue bars (bottom panels). The right panels indicate those halos which are evolving with a clustercentric distance of $r_c \geq 2r_{vir}$ at all times, while the left panels indicate those with $r_c \leq 0.5r_{vir}$ at least once.

3.3.4 Orbital parameters

In order to have an idea how orbital parameters could have related with the mass lost of the group-member halos, we calculate the eccentricity and the pericentre distance of their orbits. Physically, we might expect that galaxy mass is affected, i.e., dark matter, stars, and gas can be stripped depending of how near they are going respect to the group centre; small pericentre distances could tend to suffer greater dark matter loss. As Smith et al. (2015) carried out a comprehensive study of how orbital parameters control the strength of harassment on early-

type dwarfs in a Virgo-like cluster, finding for example that harassment is only effective at stripping stars for orbits that enter deep into the cluster core.

Thus, taking into account the importance of these parameters, we measure them by calculating the most recent pericentre and apocentre distance of the orbit of group member halos within their host and then use them to calculate the eccentricity $e = (r_{apo} - r_{peri})/(r_{apo} + r_{peri})$. We restrict this analysis to the *orbiter* group-member halos in order to test if there is a correlation between parameters of their orbits and the mass loss. Figure 3.9 shows the eccentricity (x axis) of the orbit as a function of the fractional mass loss (y axis). In the top panel all points are considered, while in the bottom they are separated according to the duration of simulations. We see that with lower values of eccentricities (< 0.2) there are lower fractions of mass lost (left side; top panel), meanwhile with more eccentric orbits the member-halos are suffering a wide range of mass loss. As points do not follow a specific trend (they are widely spread), moreover, calculating the Pearson correlation coefficients (labels in the plots), which can be interpreted as an index that can be used to measure the degree of relationship between two variables. We find that these index are different from what one would expect if there is total dependence between the two variables ($pearson = 1, -1$). This lack of a clear trend could be due to fact that the pericentre distance need to be considered. We might expected for example that more eccentric orbits with a lower pericentre distance will lead to the group-member passing close to group-centre, and therefore experiencing a stronger tidal interaction with their host's gravitational potential.

Taking into account the duration of the simulations (bottom panels with labels $2 - 6$ Gyr, $6 - 8$ Gyr), with the expectation that the simulations with longer duration might show a clearer correlation between these two parameters, as they will undergo a longer evolution. It is more that we know mass loss and length of time in the cluster or group are correlated. So we need to try and take out that dependency to see if the orbital dependency can be revealed. However, we still find a weak correlation. It seems to be that this parameter does not have a strong relation with the mass loss that the group-member halos are experiencing.

Furthermore, we take into account the pericentre distance of the orbit, which is shown in the
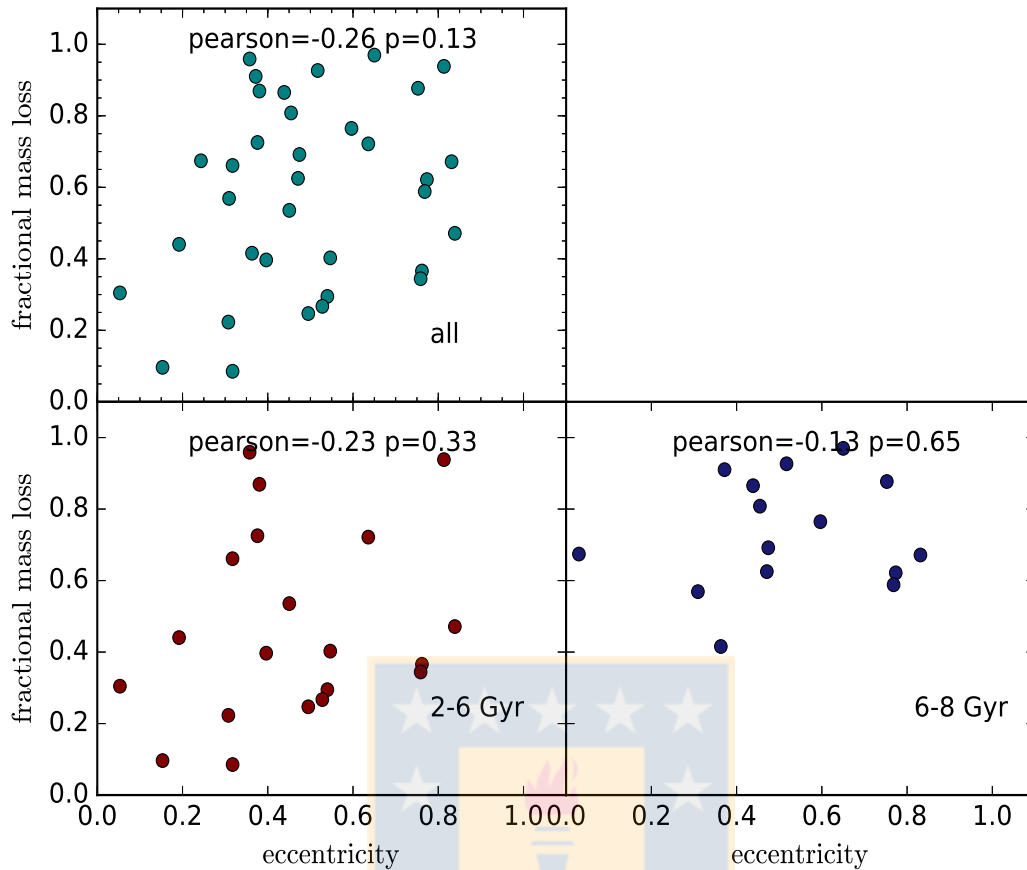
Figure 3.9: Fractional for group-member halos as a function of their orbital eccentricity. This parameter is calculated by using the latest pericentre and latest apocentre of the group-member's orbit, respect to the group centre (left top panel). Note: this panel combine all the points of the bottom panels. While these bottom panels show this relation according to the different duration of the simulations (bottom labels) for the eight clusters. While the top labels are the Pearson correlation coefficient and the p-value for each plot . Note that the low number of points in the top right panel is because we are only considering data from one cluster. Also note that this parameter is calculated only for *orbiter* group-member halos.

Fig. 3.10. This figure shows the orbital parameter; eccentricity (y axis) versus the normalised pericentre distance (x axis), wherein the colours on symbols indicate the fractional mass loss ($f_{dm} = 1 - m_f/m_i$). Group-members with smaller pericentre distances tend to have a wide range of eccentricity, and suffer high and lower fraction of mass loss. This means that this parameter alone does not have an important dependence (as we mentioned in the above paragraph), moreover the wide range of eccentricities implies that group-member halos have a large range of apocentres, which also means that halos are spending time not necessarily near to the group-centre (also related with our classification of *orbiter* and *sinker*, section 3.3.1). On the other

hand, with higher pericentre distances, the orbits tend to be more circular, but still there are higher and lower fractions of mass lost. Thereby, seem to be that orbital parameters do not have a strong dependence on the mass that group-member halos are losing. This lack of a clear trend could be due to the fact that other factors need to be considered as for example, the number of pericentre passages. This is because, with the increase in the number of pericentre passages, the mass loss could increase too. Therefore, it seems that the dark matter mass loss on group-member halos is more related to the kind of orbit within their host halo.
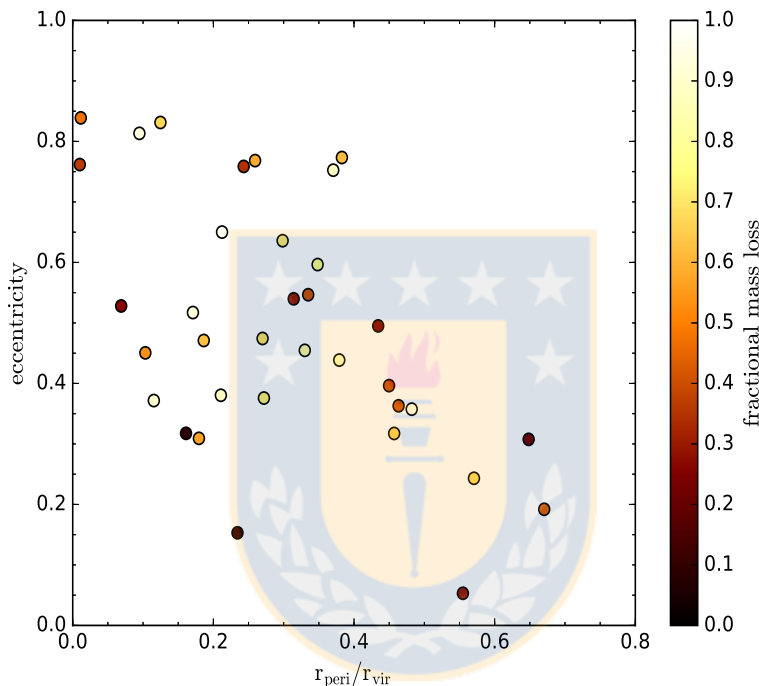
Figure 3.10: Orbital parameters as a function of the fractional mass loss of group-member halos. Eccentricity (y axis) versus normalized pericentre distance (x axis), wherein colours on symbols indicate the fractional mass loss. Note: these parameters are calculated only for *orbiter* group-member halos.

3.3.5   Relation between group and group-member mass loss

In order to investigate further the efficiency of mass loss in the group-member halos, and its relation to mass loss of the groups we plot in Fig.3.11 the fractional mass loss (f_{dm}) for groups (in the x axis) versus the fractional mass loss for group-members (in the y axis). The differ- ent symbols denote those halos evolving in (filled squares) or outside the cluster (surrounded

squares). Similarly as coloured lines show the mean group-member fractional mass loss in bins of fractional mass loss for the host groups (with one standard deviation error bars) for sinker versus orbiters (for the outside and inside cluster sample combined).

The density contours in Fig.3.11 (left panel) show that the great majority of points are situated in the upper part of plot, above the line who is denoting a 1:1 relation between the group and group-member mass loss, showing that the great majority of group-member halos have lost at least as much dark matter as their host group, whereas there are hardly any group-member halos that retain their mass when their host group mass loss is high (i.e. there is no extension of the density contours into the lower right of the plot). This suggests that the groups are generally not shielding the member halos from external tides, except for when the group-members in groups with low mass loss finally sink to the centre, as we will see later. For high mass loss groups sinking close to the centre offers no protection (there are several sinkers in the upper right corner). Furthermore, in this case, there is very little enhancement of group-member mass loss due to the group tides, as the potential wells of heavily destroyed groups are much shallower. Thus almost all the group member mass loss in the upper right of Fig.3.11 must be due to cluster tides.

On the other hand (right panel), the sinkers (orange symbols) match the mass evolution of the group much more closely than the orbiters (dark grey symbols) do (as there points are generally closer to the 1:1 line). Meanwhile the orbiters are found further away from the 1:1 line in a way that shows their group members are suffering much more mass loss than the groups they reside in. This indicates the group tides are more significant for the orbiters than on the sinkers. The physical reason for this could be that those halos which sink are now sat at the bottom of the potential well, where they do not suffer tidal stripping from the group.

Besides, there is typically a higher mass loss for group-members inside the cluster (filled squares) as well as for their host group in comparison with those ones evolving outside the cluster (surrounded squares). This suggest that tidal effects experienced inside the cluster can enhance the mass loss.
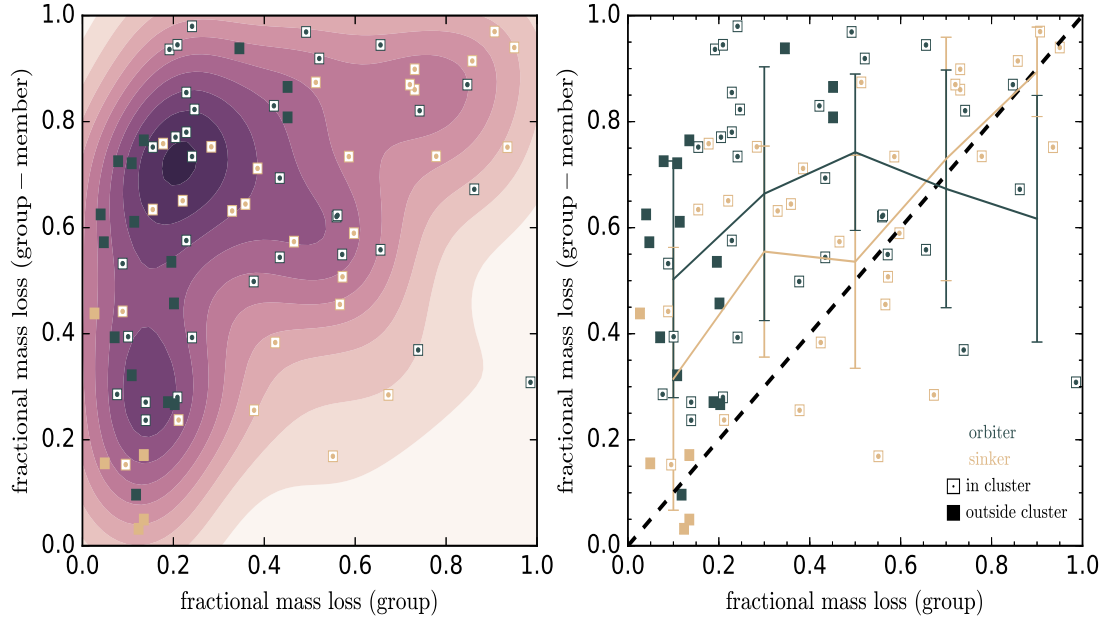
Figure 3.11: *Right:* Fractional mass loss, for group-member halos (y axis) versus group-halos (x axis). The dashed line indicates a 1:1 relation between the two. The unfilled square symbols indicate those halos which are evolving with a clustercentric distance of $r_c \geq 2r_{vir}$ at all times, while the filled squares indicate those with $r_c \leq 0.5r_{vir}$ at least once. The colour of the symbols indicates if the group-member is a sinker (orange) or an orbiter (dark grey) within the host group, meanwhile the corresponding coloured lines show the mean group-member fractional mass loss in bins of fractional mass loss for the host groups (with one standard deviation error bars) for sinkers versus orbiters (for the combined sample of halos outside and inside the cluster). *Left:* Additionally the density of points in the plot is indicated with the grey shaded contours.

3.4   Escapers group-members

From the evolution of the dark matter subhalos, we know that their trajectory depends on various internal and external factors, such as tidal effects of the group and the cluster. Furthermore, we see that a significant fraction of them do not remain associated to their host halos. After a period of time as a group-member, these halos move out of the virial radius of the group, reaching distances more than twice the virial radius as shown in Figure 3.12. In other words, this means that these halos become separated from their host: they are referred to as "escaping" halos in our classification.
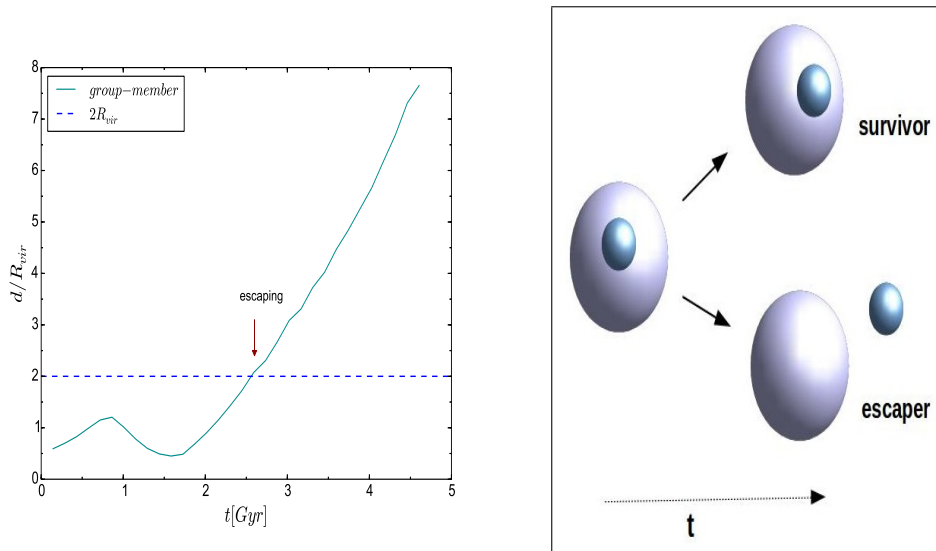
Figure 3.12: *Left:* Example of the orbit trajectory for a group-member halo that is escaping from its group. The distance is scaled to r_{vir} of the group. The horizontal line indicates a distance of $2r_{vir}$. *Right:* reminder of our classification scheme showing a group halo, and a surviving or escaping group-member halo.

3.4.1   General Properties

From the group-member halos population, we identify 122 *escaper* halos, while the others remain bound to their groups. This represents 40% of all group-members. In order to understand more about them, also because this tells us about what preprocessing may have done to galaxies, even when they are no longer in a group inside the cluster, we examine some of the general properties that these halos have at the moment they escape from the group. The left panel in Figure 3.13 is the time that these halos spend as group-members before they escape. These times are distributed in a broad range, i.e. some of the halos escape shortly after the beginning of a simulation, but others escape after spending a significant fraction of time as a member of the group.

The distribution of the fraction of mass loss that these subhalos have undergone up to the moment of escape ($f_{gm} = 1 - m(t = esc)/m_i$) are shown in the middle panel. We note that these group-member halos are distributed in a wide range of mass loss fractions, indicating that at the moment of escape, some of them have lost a high fraction of mass, while others still retain most of their mass. The right histogram (Fig. 3.13) shows the fraction of mass loss that the *groups* have at this moment ($f_g = 1 - m(t = esc)/m_i$). We again see that the

bars are distributed across the whole range of mass loss fractions, i.e. some groups have lost a small fraction of their mass, while others have lost a significant fraction of their mass when their group-members are escaping. This suggests that group member doesn't always become stripped just because the group has been destroyed or when they are losing a significant fraction of its mass.
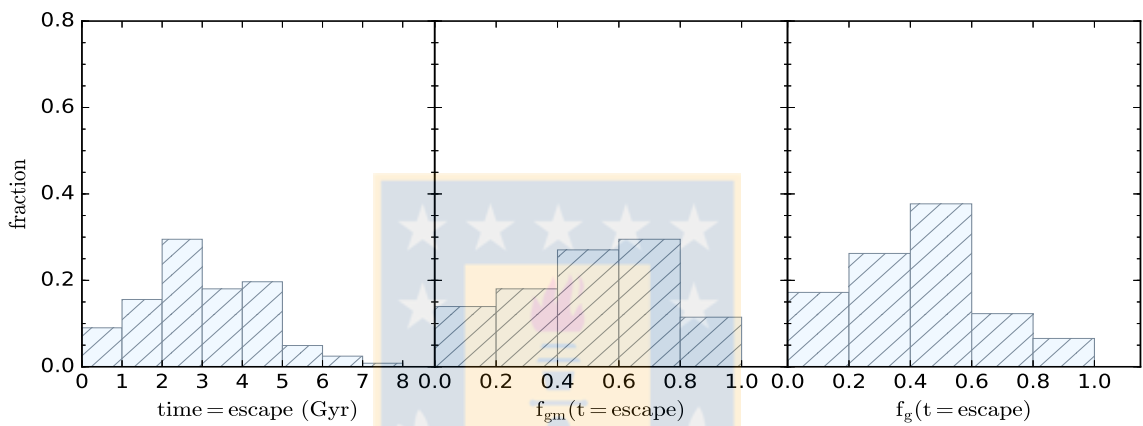
Figure 3.13: Fraction of escapers. *Left:* Time that these group-members have spent inside a group before escape ($t = escape$). *Middle:* Fractional mass loss of these group-members (f_{gm}) at the time of escape. *Right:* Fractional mass loss for the groups themselves (f_g).

3.4.2   But what determines whether a halo escapes or remains bound to the group?

We address this question by analysing different possible scenarios that could determine the behaviour of the individual escaper group-member halos in their groups.

i. **Initial distance between the group-member and the group:** Here we analyse how close the group-member halos are to the group centre, at the beginning of the simulations. The initial distance, might be expected to have a rough measure for how tightly bound the group member is to the group. Figure 3.14 shows how the distances for these subhalos scaled

to the r_{vir} of the host are distributed, for those which remain bound/surviving as a group-member (right histogram), and for those which escape (left histogram). What we see here is that even if the group-centric distance for the group-member halos that remain bound tends to be shorter in comparison to that for escaper group-members, the difference between these distance distributions is not very significant (in the sense that there is not a strong difference in the bar distributions between the two histograms). Moreover, a Kolmogorov-Smirnov (KS) test which shows if two samples are drawn from a common parent distribution, shows that the difference between the escaper and survivor distributions is quite small (as the measure of plausibility of the null hypothesis is rather slow; $p - value = 0.008$). Thus, we can said that the difference between the two distributions is not significant. Furthermore, we can say that this parameter alone is not enough to determine the subsequent evolution of the group-members within their host halo, because if a member halo is not close to the group centre, it does not necessarily mean that it will escape.
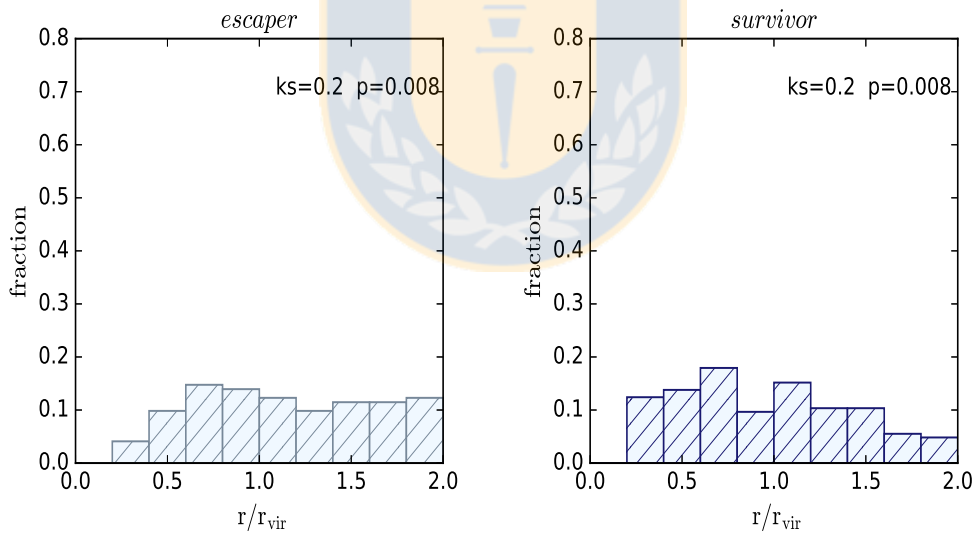
Figure 3.14: Fraction of group-member halos classified as survivors (right) and escapers (left), as a function of their initial distance with respect to their group's centre. This initial distance is scaled to the group's radius, r_{vir}. Note that $2r_{vir}$ is our distance limit to classify a halo as a member. The values on each plots indicate the statistic and the p-value when taking the KS test of the distributions.

ii. **Time when groups enter the cluster:** On the other hand, we also might expect a dependence of this factor, for example, those halos entering earlier into the cluster might be more affected for tidal effect. A consequence of this could be the stripping of some of

their subhalos. Figure 3.15 shows the cumulative fraction of group halos that have entered within a certain cluster-centric radius as a function of time since the simulation begins. The yellow line shows what fraction of groups has reached a distance of $0.25r_{vir}$ in the cluster by what time, the cyan line shows this for a distance of $0.5r_{vir}$, the blue, magenta and red lines show this for distances of $1r_{vir}$, $1.5r_{vir}$ and $2R_{vir}$ respectively. The group-member sample is split between escapers and survivors (left and right panels). We find that groups with *escaper* members enter the cluster slightly earlier, i.e. they reach these distances earlier than those groups with survivor member halos (~ 1 Gyr earlier only). For example, most of the groups with escaper members have already reached a distance of $1.5r_{vir}$ at $\sim$4Gyr, meanwhile, most of the groups with survivor members reach this distance $\sim$1Gyr later. This is made clear by the fact that the lines in the left panel of the plot are more concave than those on the right, curving up towards the upper left, indicating that a higher fraction of groups have reached each indicated distance (for a chosen fixed time) than in the right panel. This suggests that, for those groups entering earlier into the cluster, we would expect that the tides of the cluster environment have more time to remove the group-members of these groups, as they are losing more mass inside the cluster environment. The difference between the two plots is not, however, substantial[4] and so, it appears that even if the host groups in the are spending slightly more time inside the cluster and losing more mass due to cluster tides, it does not necessarily mean that their group-members will escape. This is shown more clearly in the next section (item iii).

iii. **Mass loss of groups (and time entering in the cluster):** To understand in more detail the previous possible cause of group-members to escape, we also consider if the mass loss of the groups has an important role controlling the outcome. We might expect that groups losing a high fraction of their masses, might have members who are more easily stripped. The left panel of Figure 3.16 shows the final fractional mass loss of groups as

---

[4]A (KS) test on the two samples, shows that there is a difference between the cumulative distributions in both sub-samples. However, when taking a KS test of the time distributions (histograms) of the two samples, the difference is not significant.
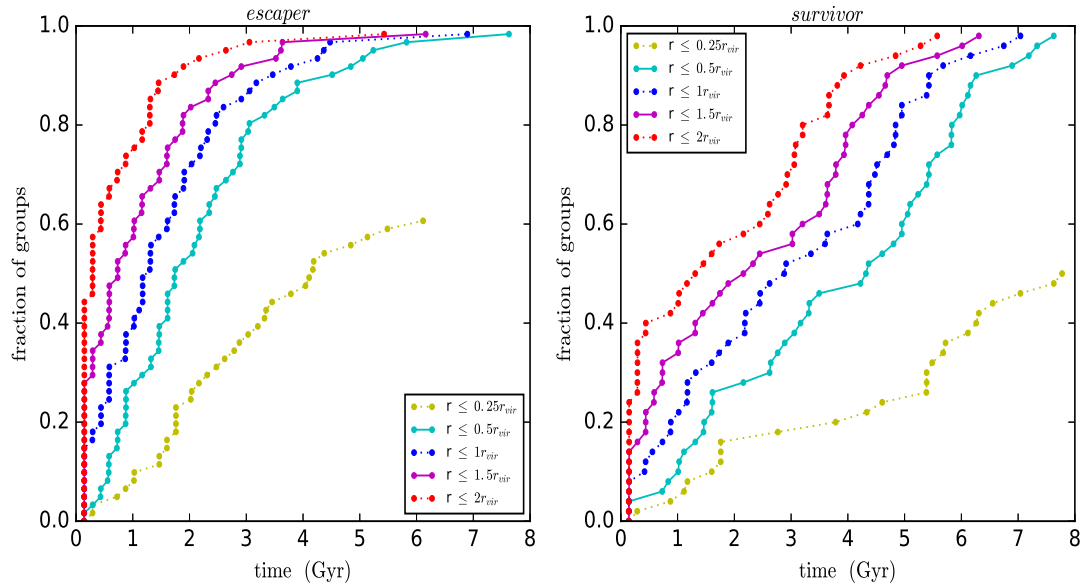
Figure 3.15: Cumulative fraction of group halos that reach different distances in the cluster during cluster infall, for groups with escaper group-members (left) and for groups with survivor group-members only (right). The yellow line shows the time and fraction of groups that have reached a distance of $0.25r_{vir}$, the cyan line shows this for a distance of $0.5r_{vir}$ in the cluster, the blue, magenta and red lines show this for the distance of $1r_{vir}$, $1.5r_{vir}$ and $2r_{vir}$ respectively. The coloured dots over the lines mark the fraction of groups reaching these distance at different times.

a function of the time when those groups enter a distance of $0.5r_{vir}$ in the cluster. Here the vertical lines indicate that multiple groups may reach this distance at the *same time*, and the symbols denote groups with an escaper group-member (white triangle) and groups with a survivor group-member (blue dots). Interestingly, while we do find that groups lose more mass if they have been in the cluster longer (we corroborate this by checking some groups who show this behaviour, i.e., the more time they spend inside or near to the cluster centre, they lose more mass) and so, an infall of only 1 Gigayear earlier (as we showed before in Figure 3.15) is not enough to turn many survivor group-members into escaper group-members. For example, we can see (left panel) that group halos losing more than 80% of their masses (left top part) are reaching this distance in the cluster earlier, whereas those groups losing less than 40% of their masses are reaching this distance later (right bottom part). In fact, although the groups lose more mass if they are longer in the cluster, they still contain both escapers and survivors, as is shown in the histogram in the right panel. This shows the fractional mass loss for groups containing only survivors and those with escapers. Groups with a high fraction of mass loss still have some survivor

group-members, and groups losing little mass have escaping group-members. This means that whether a group-member finishes as a survivor or escaper is not a sensitive function of the time of infall, or the amount of mass the group has lost.
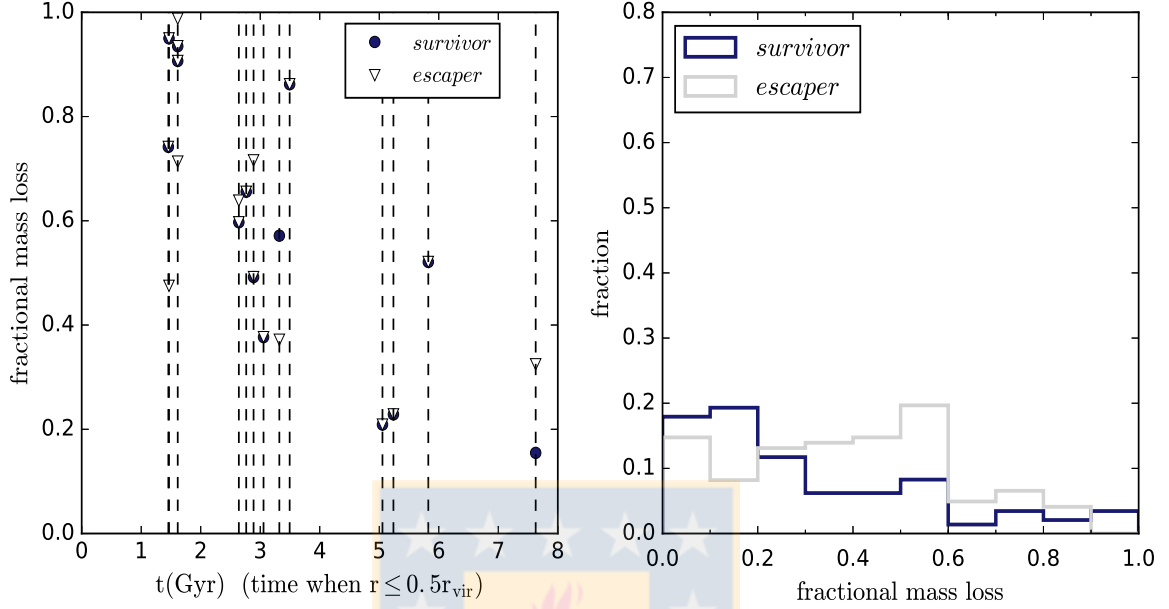

Figure 3.16: *Left:* Group-member behaviour as a function of the fractional mass loss of the group (y-axis) and the time of entry within $0.5r_{vir}$ of the cluster-centric distance (x-axis). The vertical lines denote groups reaching this distance at the same time, and the symbols illustrate groups with escaper group-members (white triangles) and groups with survivor group-members (blue dots). Note that a blue dot over a white triangle means that the same group has both escaper and survivor group-members *Right:* Histogram of the fractional mass loss distribution for groups with survivor and escaper group-members.

iv. **Distance of the group-member within the group, when the group first passes cluster pericentre:** The histograms in Figure 3.17 show the distribution of the distances (scaled to the r_{vir} of the group) that the group-member halos have within their groups, at the moment of first pericentric passage within the cluster, for surviving (right) and escaping group-members (left). We see that there is a large fraction ($\sim 50\%$) of *survivor* group-members at smaller distances (i.e. less than $0.2r_{vir}$) as compared with the *escaper* distribution, which is more broad. As the two distributions differ significantly, we can see that group-members that are further away from the centre of the group at this moment (group pericentric passage), are more able to escape in comparison with those lying closer to the group's centre. This suggests that the tides of the cluster are much more effective in

"removing" those group-member halos which are orbiting in the outer regions of the group, as there they are more susceptible to the cluster tides. In addition, only $\sim 10\%$ of the total population of groups with escaper group-member halos are evolving outside the cluster, so clearly this is an important factor. Alternatively, it is clear from the right hand histogram of survivor group-members, that they lie very close to the centre of their host, and so are to some extent protected from the tidal effect of the cluster. Also, as we mentioned in Section 3.3.3, most of the survivor group-members sink into the centre of their group halo.
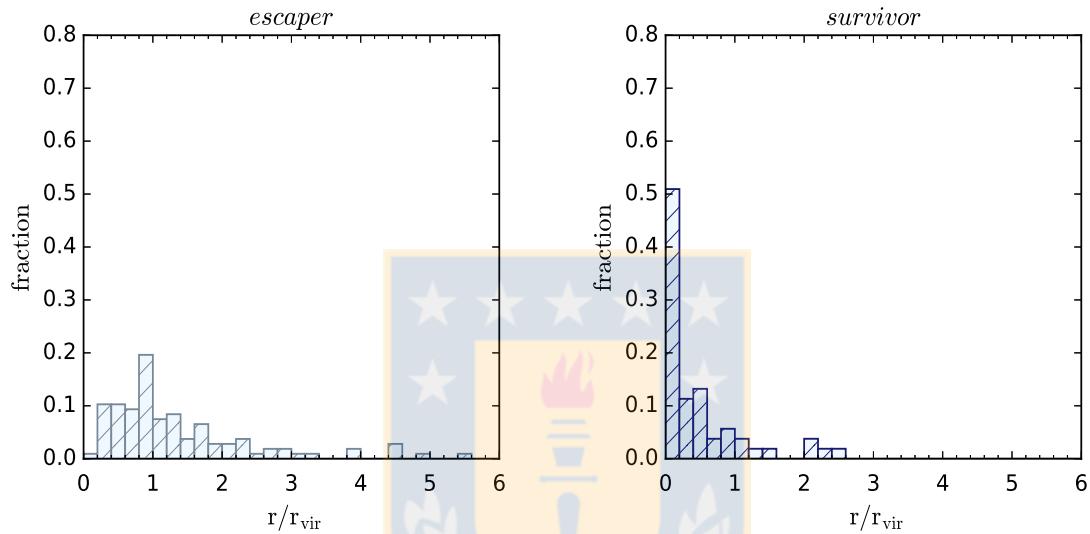
Figure 3.17: Distribution of the distances, scaled to the r_{vir} of their host group, that the group-member halos have within their groups. This distance is measured when the host groups are at first pericentric passage in the cluster. The left panel shows this distribution for group-member halos that escape, and the right panel for those that survive in the group.

Additionally, we might expect also a dependence of the pericentre distance of the groups within the cluster, i.e., presumably those passing very close to pericentre can have much more "embedded" halos that escape, than groups that have less close passages. To explore this, we present the Figure 3.18 which is showing the same distributions of distances that group-members have within their host group (same Fig. 3.17), but now also considering the pericentre distance of groups within the cluster (colours in bars). We see in the distribution for groups with escaper members (left panel) that in most of the bins there is a significant percentage of groups with a closer pericentre distance within the cluster ($r_{peri}/r_{vir} < 0.25$). On the other hand, the other distribution (right panel) shows that groups tend to have

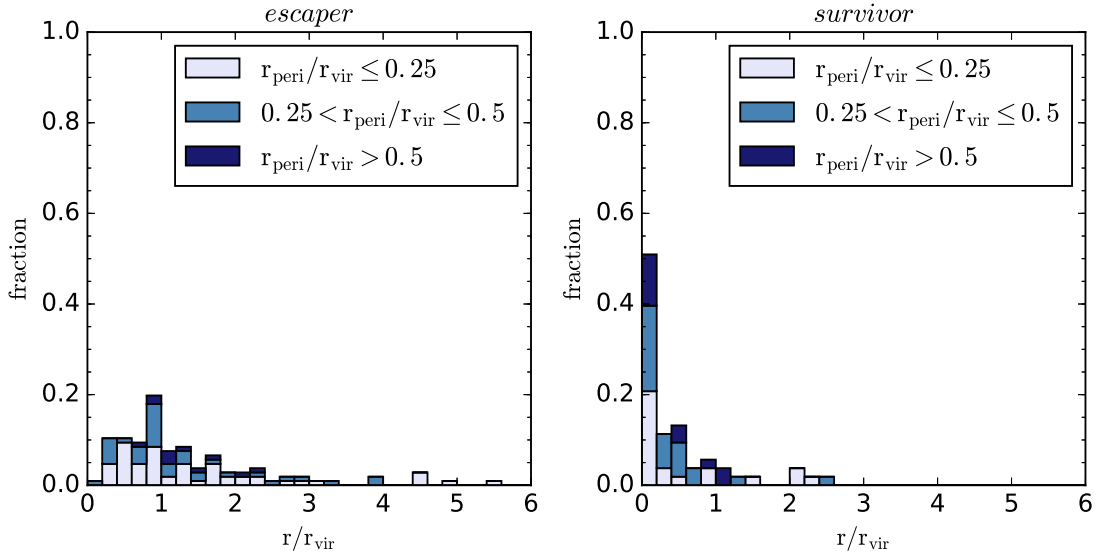Figure 3.18: Distance (scaled to the r_{vir}) of the group-member within the group, when the group first passes cluster pericentre. This is shown for "escaper" (left) and "survivor" (right) member halos. Note: the colours in bars are denoting the normalized pericentre distances of groups within the cluster (r_{peri}/r_{vir}).

larger distances, particularly in the bars with higher fraction of survivors. Although, the difference between the two distributions is not significant. This suggests that groups passing closer to the cluster centre could have more "embedded" halos that escape. This occurs (as we said in the previous paragraph) because they are more susceptible to the tidal effect of the cluster, and as a consequence, group-member halos could be stripped from their host halos.

The subsequent evolution of individual group-member halos, in particular, the possibility to escape from the host group, appears to be strongly connected to the group-member distance within the group at the moment of the group's pericentric passage within the cluster.

The larger separation of escaper group-members from the centre of their group hosts is further supported by applying our "orbiter" and "sinker" classifications to the survivor and escaper subsamples. In Fig. 3.19 we illustrate the division of the survivor and escaper subsamples into orbiters and sinkers. We can see that 100% of the group-member halos escaping from their host group (left hand side pie chart) are in fact those halos that are classified as "orbiters", i.e. they are not sinking close to the group centre. In the case of the survivor group-members,

however, $\sim 69\%$ are orbiters, whereas the remainder are sinkers. Thus the majority of the group-member halos of the survivor subsample are orbiters, implying that the large fraction of survivor subhalos with group-centric distances $< 0.2r_{vir}$ is not simply due to a dominant population of sinker halos. This lends further support to the statement that the group-centric distance of the group-member halo at pericentric passage of the group in the cluster is a crucial parameter determining the probability of escape.

Furthermore, the fact that the escaper subhalos are all orbiters, and we have shown that orbiter group-member halos tend to lose more mass (relative to the group mass loss) as they are more susceptible to the group tides, implies that the groups are releasing their more damaged member-halos into the cluster. This is also related with the fact that a high fraction of the orbiter group member-halos are classified as destroyed (i.e. their mass goes below the resolution limit of the simulation) as we see in Fig.3.20. Therefore, it appears that groups tend to retain their least damaged halos, as the sinkers are always classified as survivors, and these group-members halos are generally more protected from further effects of the group tides. The more tidally damaged group-member halos, however, are being released into the cluster. It should be borne in mind, however, that almost 70% of the surviving group-member halos are orbiters, and will therefore also have suffered tidal disruption due to the group.

Although our study utilises a simulation without baryons, it is nevertheless interesting to try to place these results in the context of galaxy evolution. Given that the dark matter halos of escaping group-members tend to have been heavily stripped, this could indicate that some heavily tidally disrupted cluster galaxies were damaged in their previous group environment. Therefore, our study lends support to the notion of groups populating a cluster with heavily pre-processed galaxies.
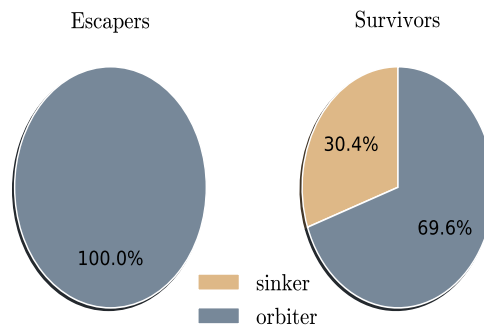
Figure 3.19: Percentages of escaper (left) and survivor (right) group-member halos, that are sinker (yellow) or orbiters (grey), according to our classification.
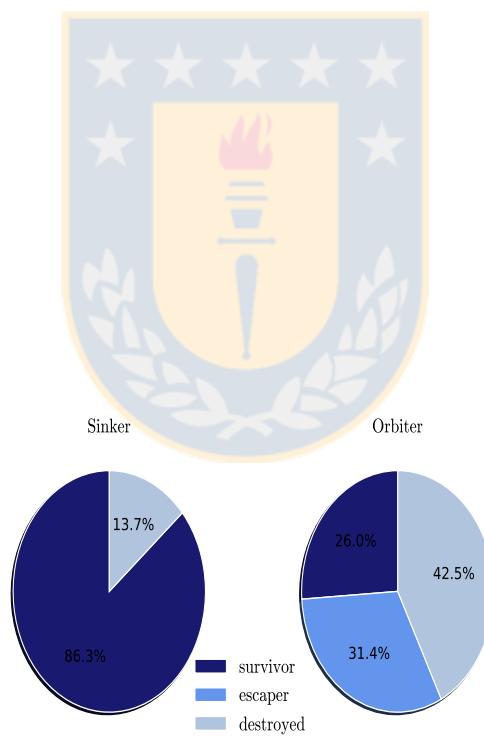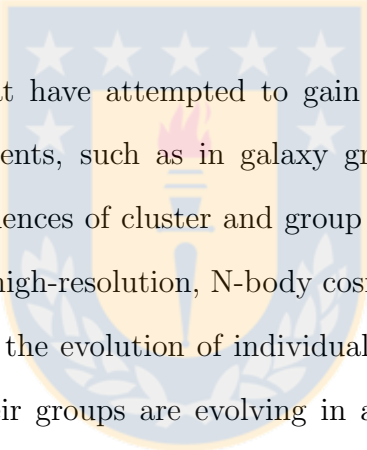

Figure 3.20: Percentages of sinker (left) and orbiter (right) group-member halos. The different blue colours denote the percentages of survivor (dark), escaper (middle), and destroyed (light) member halos. See section 2.3.1.

Chapter 4

Discussion and Conclusions

Motivated by several studies that have attempted to gain more insights into the evolution of galaxies in different environments, such as in galaxy groups and/or galaxy clusters, we performed a study of the consequences of cluster and group environments on the evolution of galactic dark matter halos using high-resolution, N-body cosmological simulations. In order to carry out this study, we followed the evolution of individual group-member halos, identifying what happens to them while their groups are evolving in and around the cluster and what parameters control the outcome of their evolution. As previous studies have suggested, during the cluster accretion process, a significant fraction of galaxies enter the cluster within groups. In this context, certain mechanisms are triggered on galaxies that are caused not only by the cluster environment but also by the group, particularly when the galaxy spends a long time in the group environment prior to falling into the cluster. In this analysis, comparing the initial number of group halos (plus their members) to the total number of halos, we found that the sample corresponds to ~ 11 per cent of the total halos on each cluster. Moreover, we found that the surviving group-member halos correspond to 32% of the total number of group member halos, meanwhile those escaping from their host correspond to $\sim 27\%$. In this way we stress an important dependence on the environment where the DM halos are evolving, and which is causing this outcome.

4.1   The role of pre-processing

In the hierarchical scenario for structure formation, halos first form as small objects and then grow more massive over time. In this context cluster galaxies may have previously resided in smaller systems such as galaxy groups, before accretion into a cluster, leading to a pre-processing stage in the evolution of galaxies within these smaller systems (Cortese et al., 2006; Vijayaraghavan & Ricker, 2013). This stage in the galaxy evolution process has been widely discussed in the analysis of simulations, wherein several studies point out that a significant percentage of galaxies that were accreted into a cluster did so as part of a group. For example McGee et al. (2009) estimate that $\sim 25\%$ of galaxies accreted into clusters with masses $10^{14.5}h^{-1}M\odot$ have done so within group halos of mass $10^{13}M\odot$, rising to $\sim 40\%$ in more massive clusters. Also (De Lucia et al., 2012) estimate similar percentages considering a cluster-size halo with $\sim 10^{14}M\odot$. Both analyses suggest that, as galaxies spent a significant fraction of time as satellites in smaller systems before becoming part of the cluster, they are being "pre-processed". In this context our analysis is in agreement with these previous studies (even if we are considering lower mass group halos) as we find that a significant fraction of our sample of galactic dark matter halos are being accreted as groups into larger cluster-sized halos with masses $\sim 10^{14}M\odot$. Therefore, as in previous works, we stress the importance of the environment in the evolution of galaxies. Although these previous studies are focused in to measure the fraction of these galaxies, this study was focused on what the actual effect on the galaxies is. Actually, more specifically, the effect on their dark matter halos. As we mentioned previously there is a a non-negligible fraction of halos in our cluster sample that are entering to the cluster as a member of a larger halos.

Thereby, our study also suggests the importance of the pre-processing stage, as we find that group-member halos evolving within group halos that have yet to enter the cluster are affected primarily by the group environment (section 3.2.2). When analysing how they are losing dark matter mass, in some cases we find a high fraction of mass loss in the group-members, and the tides of the group seem to be the main factor responsible. Several previous observational studies have analysed galaxies at this stage in their evolution, showing evidence of the baryonic

content being affected, principally the star formation (e.g Cortese et al., 2006).

Galaxies that fall into a cluster as a member of a group are not, however, immediately dissociated, as we also pointed out in the section 3.4, most of the group-member halos become escapers after first pericentre passage of groups, in this sense until this moment they are affected by the combined cluster and group environment. In addition, the gas and dark matter associated with an infalling group interacts with the cluster material, affecting the local environment (*post-processing*). In this line, we find that the dark matter mass loss increases when the group and group-member halos enter the cluster environment, and that the group continues to have an effect on its group-members within the cluster. Additionally, in figure 3.2 we showed that not all isolated halos are losing a high fraction of their masses, in comparison with those halos within a host group (which typically tend to increase their mass loss when entering the cluster). This, is indicating that groups have a strong effect on their member halos.

Our results stress the importance of pre-processing in the evolution of a cluster galaxy, even if we are considering in this analysis only the dark matter component. Obviously it would be desirable to do a complete analysis of a cosmological simulation that includes baryons, as then we could investigate both the dynamics of the group galaxies and the effects of the tidal interactions on the baryonic component. But the link between the dark matter and baryons as has been suggested by other studies which claim that effects on the baryonic configuration appear to in cases with the strongest dark matter mass loss. For example more than $\sim 80\%$ of the dark matter halos had to be stripped before see any removal of stars, as they are embedded deeply within the potential well of their galaxy's dark matter halo (Peñarrubia, Navarro & McConnachie, 2008; Smith et al., 2015). Moreover, it is assumed (statistically) that the more dark matter was lost by a given subhalo over time, the more its stellar structure was tidally heated, leading to thickening or even destruction of disks and causing mild to strong stellar mass loss (Mastropietro et al., 2005; Smith, Davies & Nelson, 2010). Additionally morphological transformation from disc in spheroids, dynamical heating causing enhanced dispersion and reduced rotation (Aguerri & González-García, 2009)

4.2   Environmental dependence

Several previous studies, through the analysis of simulations and/or observations, have shown evidence for how galaxies are affected while they are evolving in denser systems, wherein their morphology and internal structure are affected. Moreover, some of these consequences seem to be associated particularly with the group environment, due to a high fraction of cluster galaxies being accreted within groups. In our study we have analysed how the evolution of galactic dark matter halos is affected by the influence of both the group and cluster environments.

In order to estimate the efficiency of this environmental dependence in galaxy evolution, we have analysed the mass loss that the DM halos suffer, with the expectation that this is a proxy for the full consequences of the environmental influence on a galaxy. We have shown in the section 3.2.1 that this stripping process in the outer cluster regions is diminished, as we find that groups and group-member halos orbiting inside the virial radius of the cluster suffer a higher fraction of mass loss than those evolving in the outer cluster regions, suggesting that the cluster tides cause this increase in the amount of dark matter stripping. Nevertheless, the fact that some substantial mass loss is also seen in group-member halos orbiting within their host groups outside the cluster, prior to accretion, suggests the importance of the *pre-processing* effect. The fact that there is an enhancement of group-member mass loss once inside the cluster is also supportive of the *post-processing* effect.

This is in agreement with other studies, such as De Lucia et al. (2012), who analysed the evolution with time of the stripping process, finding that once a subhalo is accreted by a larger system, tidal stripping is highly effective, and that moreover the longer a substructure spends in a more massive halo, the larger is the destructive effect. Similar studies, such as Lisker et al. (2013), have analysed the mass loss and infall history of subhalos in massive clusters (from the Millennium-II simulation, Springel et al., 2005) making a connection with the baryonic content of galaxies, and in particular analysing the history of the present-day dwarf galaxy population in the Virgo and Coma clusters. Their main results point out that if a subhalo loses a substantial amount of its mass over time, then the baryonic content (gas and stars) is affected noticeably, and only in cases with strong subhalo mass loss can the baryonic configuration of the galaxy

be affected significantly. Additionally, Smith et al. (2015) found that a high percentage ($\sim$ 85%) of dark matter need to be stripped before see any removal of globular clusters and stars of early-type dwarf galaxies. In this sense, we also expect that a strong stripping of the dark matter content on the group-member halos should imply a stripping of the baryonic content.

When analysing the history of group-member halos to interpret the mass stripped from them, we must also consider the kind of orbit that they have within their host. As we have shown (section 3.3.1), those halos that sink close to the center of their host due to dynamical friction become tied to the fate of their host halo. Meanwhile, those not having this kind of orbit, tend to lose more mass as they are more susceptible to the group tides while they are orbiting.

Note that those halos sinking very close to the center of their host halo would, in a more complete physical interpretation, most likely be considered a galaxy merger. Obviously we cannot observe the whole process and confirm this, as we are limiting our analysis only to DM halos. It is nevertheless interesting to note that when this happens, the halos are not disrupted immediately in the process. It would be desirable to confirm these mergers with an analysis using simulations that include the baryonic component. Actually simulations of galaxy mergers including baryons are very common (e.g. the Galmer database), but it would be interesting to test under what circumstances a merger occurs, and the substructure remains a bound entity. In fact, a search of the Galmer database for this might also be possible.

Another major conclusion of the present thesis relates to the possible cause(s) for some group-member halos to escape from their host group: our results suggest that the most important factor is the group-member's distance from the centre of its host group at the moment of the group's pericentre passage within the cluster. This scenario appears to be supported by the fact that groups at the first pericentre passage within the cluster are more susceptible to the cluster tides, and so their group-member halos are also susceptible to these tides, which are more effective on halos further from the group centre at this moment and consequently they are stripped from their hosts. In this sense, subhalos with very eccentric orbits might be more likely to be stripped, as galaxies spent most of their time at apocentre. Additionally clearly loose groups should be more disrupted than compact groups. Therefore, contrary to expectations,

the mass loss experienced by the host groups is usually not the most important factor leading to the escape of group-member halos. It is also possible to observe in the simulations halos that still remain as a group-member inside their host groups, even if those groups have lost a high fraction of mass. In the general context of galaxy evolution, this result could serve as a clue to help understand the histories of some cluster galaxies, as they may have been "expelled" from their groups due to the process we have studied here, and so preprocessed galaxies could be mixed in with the general cluster population. Another important element in this process could be the overall gravitational accelerations associated to tides caused by the other halos, as well as the tides caused by the cluster. A measurement of the full tidal forces experienced by groups and group-member halos would help in the determination of the relative importance of the cluster and other substructure in triggering the separation of the halos from their hosts. Moreover, doing a rough check shows that tides caused for other halos could have an important effect.

To fully understand the group and/or cluster effect on galaxy evolution, would be desirable to do this analysis with a larger sample of clusters. In this way, the statistics would be more robust, as well as our speculations.

4.3   Summary

In order to address the questions posed at the beginning of this thesis, we carried out an analysis of simulations of dark matter halos in order to get more insights into the effects of the cluster and group environments on the evolution of galaxies. We followed the evolution of individual group-member halos, and attempted to identify the main parameters controlling the outcome of their evolution, principally in terms of the dark matter mass loss that they experience, and the main factors permitting some of them to escape from their host halos. The analyses in this thesis have resulted in general conclusions which we now summarize.

- Group member halos suffer a wide range of dark matter mass loss, from very weak (less than 10%) to very strong (more than 90%). Many lose a high fraction of their mass, even

if they never enter the cluster, which highlights that the tidal field within groups can be very important for the mass loss of some cluster galaxies.

- We find that the strength of dark matter mass loss is dependent on the orbital behaviour of the group member within their host group. Those that sink close to the centre of the group halo tend to lose less dark matter, and their fate becomes similar to the mass loss of the group halo. Meanwhile those that avoid sinking are more susceptible to the group tides, and lose more mass.

- One of the main factors deciding whether a group member escapes from its host group is the radial distance from the centre of the group halo when the group passes cluster pericentre. Other factors, such as time within the cluster and group mass loss appear to be less important parameters in deciding when a group-member halo escapes. The underlying physical reason for this importance of the group-centric distance at this moment is that the group-member is more susceptible to the cluster tides if it is located far from the protective centre of its host group, and consequently it is easier to strip from the host. This result could give us insights into the histories of cluster galaxies, with some galaxies possibly having been "expelled" in this manner. So mixing in preprocessed galaxies with the general cluster population

- Thereby, in agreements with the above conclusions, The results above imply that galaxy groups tend to maintain their least damaged group members, while realising their most tidally damaged members into the cluster. Therefore, galaxy groups can effectively pollute the cluster population with preprocessed galaxies that are no longer associated with their former groups.

The conclusions of this thesis stress the importance of the role that the group and cluster environments have in galaxy evolution. In this study we have limited the analysis to the dark matter content of galaxies. Clearly, a more comprehensive analysis of simulations that include the baryonic material of the galaxies would be desirable and will likely provide further important clues to understand the consequences of differing environments. In addition, such an analysis

would provide crucial insights for observational studies of galaxy evolution and environmental dependence.

Bibliography

Aarseth S. J., 1963, MNRAS, 126, 223

Aguerri J. A. L., González-García A. C., 2009, aap, 494, 891

Alimi J.-M. et al., 2012, ArXiv e-prints

Balogh M., Bower R. G., Smail I., Ziegler B. L., Davies R. L., Gaztelu A., Fritz A., 2002, MNRAS, 337, 256

Benson A. J., 2010, PhR, 495, 33

Bett P., Eke V., Frenk C. S., Jenkins A., Helly J., Navarro J., 2007, MNRAS, 376, 215

Boselli A., Gavazzi G., 2006, pasp, 118, 517

Bouchard A., Da Costa G. S., Jerjen H., 2009, AJ, 137, 3038

Bullock J. S., 2010, ArXiv e-prints

Carollo C. M. et al., 2013, ApJ, 776, 71

Cole S., Lacey C. G., Baugh C. M., Frenk C. S., 2000, MNRAS, 319, 168

Corbelli E., Salucci P., 2000, MNRAS, 311, 441

Cortese L., Gavazzi G., Boselli A., Franzetti P., Kennicutt R. C., O'Neil K., Sakai S., 2006, AAP, 453, 847

De Lucia G., Weinmann S., Poggianti B. M., Aragón-Salamanca A., Zaritsky D., 2012, MNRAS, 423, 1277

Dehnen W., Read J. I., 2011, European Physical Journal Plus, 126, 55

Di Matteo T., Springel V., Hernquist L., 2005, natur, 433, 604

Dressler A., 1980, ApJ, 236, 351

Ebeling H., Stephenson L. N., Edge A. C., 2014, apjl, 781, L40

Fujita Y., 2004, pasj, 56, 29

Gill S. P. D., Knebe A., Gibson B. K., 2004, mnras, 351, 399

Gunn J. E., Gott, III J. R., 1972, ApJ, 176, 1

Jiang F., van den Bosch F. C., 2014, MNRAS, 440, 193

Kazantzidis S., Moore B., Mayer L., 2004, in Astronomical Society of the Pacific Conference Series, Vol. 327, Satellites and Tidal Streams, Prada F., Martinez Delgado D., Mahoney T. J., eds., p. 155

Klypin A., f A. V., Valenzuela O., Prada F., 1999, ApJ, 522, 82

Klypin A. A., Trujillo-Gomez S., Primack J., 2011, ApJ, 740, 102

Knebe A., Gill S. P. D., Gibson B. K., 2004, pasa, 21, 216

Knebe A., Green A., Binney J., 2001, mnras, 325, 845

Knebe A. et al., 2013, MNRAS, 435, 1618

Knobel C. et al., 2013, ApJ, 769, 24

Koch A., Burkert A., Rich R. M., Collins M. L. M., Black C. S., Hilker M., Benson A. J., 2012, ApJ, 755, L13

Lewis I. et al., 2002, MNRAS, 334, 673

Lisker T., Weinmann S. M., Janz J., Meyer H. T., 2013, mnras, 432, 1162

Lynden-Bell D., 1967, mnras, 136, 101

Mastropietro C., Moore B., Mayer L., Debattista V. P., Piffaretti R., Stadel J., 2005, mnras, 364, 607

McGee S. L., Balogh M. L., Bower R. G., Font A. S., McCarthy I. G., 2009, MNRAS, 400, 937

Merchán M. E., Zandivarez A., 2005, ApJ, 630, 759

Merritt D., Navarro J. F., Ludlow A., Jenkins A., 2005, ApJ, 624, L85

Mo H., van den Bosch F. C., White S., 2010, Galaxy Formation and Evolution

Moore B., Ghigna S., Governato F., Lake G., Quinn T., Stadel J., Tozzi P., 1999a, ApJ, 524, L19

Moore B., Lake G., Quinn T., Stadel J., 1999b, MNRAS, 304, 465

Navarro J. F., Frenk C. S., White S. D. M., 1996, ApJ, 462, 563

Navarro J. F., Frenk C. S., White S. D. M., 1997, ApJ, 490, 493

Navarro J. F. et al., 2004, MNRAS, 349, 1039

Navarro J. F., White S. D. M., 1994, MNRAS, 267, 401

Padmanabhan T., 1993, Structure Formation in the Universe. p. 499

Peñarrubia J., Navarro J. F., McConnachie A. W., 2008, Astronomische Nachrichten, 329, 934

Pfeffer J., Baumgardt H., 2013, MNRAS, 433, 1997

Planck Collaboration et al., 2015, ArXiv e-prints

Poggianti B. M. et al., 2001, ApJ, 562, 689

Poggianti B. M. et al., 2008, ApJ, 684, 888

Read J. I., Wilkinson M. I., Evans N. W., Gilmore G., Kleyna J. T., 2006, MNRAS, 366, 429

Rubin V. C., Ford W. K. J., . Thonnard N., 1980, ApJ, 238, 471

Sawala T., Guo Q., Scannapieco C., Jenkins A., White S., 2011, MNRAS, 413, 659

Schaye J. et al., 2015, MNRAS, 446, 521

Smith R., Davies J. I., Nelson A. H., 2010, MNRAS, 405, 1723

Smith R. et al., 2015, mnras, 454, 2502

Somerville R. S., Davé R., 2015, ARAA, 53, 51

Springel V. et al., 2008, MNRAS, 391, 1685

Springel V. et al., 2005, Natur, 435, 629

Taylor J. E., Babul A., 2004, mnras, 348, 811

Toloba E. et al., 2016, ApJ, 816, L5

Toomre A., Toomre J., 1972, ApJ, 178, 623

Tormen G., Bouchet F. R., White S. D. M., 1997, MNRAS, 286, 865

van den Bosch F. C., Aquino D., Yang X., Mo H. J., Pasquali A., McIntosh D. H., Weinmann
    S. M., Kang X., 2008, MNRAS, 387, 79

Vijayaraghavan R., Ricker P. M., 2013, MNRAS, 435, 2713

Vogelsberger M. et al., 2014a, MNRAS, 444, 1518

Vogelsberger M. et al., 2014b, mnras, 444, 1518

Warnick K., Knebe A., 2006, MNRAS, 369, 1253

Weinmann S. M., Kauffmann G., van den Bosch F. C., Pasquali A., McIntosh D. H., Mo H.,
    Yang X., Guo Y., 2009, MNRAS, 394, 1213

White S. D. M., Rees M. J., 1978, MNRAS, 183, 341

Yang X., Mo H. J., van den Bosch F. C., Jing Y. P., 2005, MNRAS, 356, 1293

Ziparo F. et al., 2014, MNRAS, 437, 458